






Targeting epigenetic regulation and post-translational modification with 5-Aza-2' deoxycytidine and SUMO E1 inhibition augments T-cell receptor therapy

Jessie S Kroonen ¹, Anne K Wouters,² Ilona J de Graaf,¹ Dennis F G Remst,² Sumit Kumar,¹ Tassilo L A Wachsmann ², Amina F A S Teunisse,¹ Jessica P Roelands,³ Noel F C C de Miranda ³, Marieke Griffioen,² Mirjam H M Heemskerk ², Alfred C O Vertegaal ¹

To cite: Kroonen JS, Wouters AK, de Graaf IJ, *et al.* Targeting epigenetic regulation and post-translational modification with 5-Aza-2' deoxycytidine and SUMO E1 inhibition augments T-cell receptor therapy. *Journal for ImmunoTherapy of Cancer* 2024;**12**:e008654. doi:10.1136/jitc-2023-008654

► Additional supplemental material is published online only. To view, please visit the journal online (<https://doi.org/10.1136/jitc-2023-008654>).

This paper is dedicated to the memory of our colleague Mr. Edwin Willemstein, who sadly passed away on July 10th 2020 at the age of 26, after a brave and hard battle with AML. Edwin was a talented technician and a highly valued member of the Vertegaal team.

MHMH and ACOV are joint senior authors.

Accepted 07 June 2024



© Author(s) (or their employer(s)) 2024. Re-use permitted under CC BY-NC. No commercial re-use. See rights and permissions. Published by BMJ.

For numbered affiliations see end of article.

Correspondence to

Alfred C O Vertegaal;
vertegaal@lumc.nl

Mirjam H M Heemskerk;
m.h.m.heemskerk@lumc.nl

ABSTRACT

Background Cellular immunotherapy using modified T cells offers new avenues for cancer treatment. T-cell receptor (TCR) engineering of CD8 T cells enables these cells to recognize tumor-associated antigens and tumor-specific neoantigens. Improving TCR T-cell therapy through increased potency and in vivo persistence will be critical for clinical success.

Methods We evaluated a novel drug combination to enhance TCR therapy in mouse models for acute myeloid leukemia (AML) and multiple myeloma (MM).

Results Combining TCR therapy with the SUMO E1 inhibitor TAK981 and the DNA methylation inhibitor 5-Aza-2' deoxycytidine resulted in strong antitumor activity in a persistent manner against two in vivo tumor models of established AML and MM. We uncovered that the drug combination caused strong T-cell proliferation, increased cytokine signaling in T cells, improved persistence of T cells, and reduced differentiation towards exhausted phenotype. Simultaneously the drug combination enhanced immunogenicity of the tumor by increasing HLA and co-stimulation and surprisingly reducing inhibitory ligand expression.

Conclusion Combining T-cell therapy with TAK981 and 5-Aza-2' deoxycytidine may be an important step towards improved clinical outcome.

INTRODUCTION

Immunotherapies have significantly improved over the past decades. T-cell receptor (TCR) engineering of T cells is one of the immunotherapeutic strategies whereby patient's own T cells are engineered ex vivo to express a tumor-targeting TCR before being reinjected into the patient.^{1 2} Tumor targeting TCR T cells can either recognize neoantigens derived from mutations that are unique to the tumor or tumor-associated antigens which are elevated in tumor tissues.

WHAT IS ALREADY KNOWN ON THIS TOPIC

⇒ T-cell receptor (TCR) engineering of CD8 T cells enables these cells to specifically recognize tumor cells.

WHAT THIS STUDY ADDS

⇒ Combining TCR therapy with the SUMO E1 inhibitor TAK981 and the DNA methylation inhibitor 5-Aza-2' deoxycytidine yielded strong antitumor activity in a persistent manner against two in vivo tumor models of acute myeloid leukemia and multiple myeloma.

HOW THIS STUDY MIGHT AFFECT RESEARCH, PRACTICE OR POLICY

⇒ Combining T-cell therapy with TAK981 and 5-Aza-2' deoxycytidine may enhance the clinical efficacy of TCR therapy.

These tumor antigens are presented to T cells by major histocompatibility complex (MHC) class I, and recognition of these antigens by T cells can result in direct lysis of tumor cells.^{3–5}

While this approach has demonstrated early clinical potential, challenges remain regarding the efficacy and persistence of the transferred T cells.¹ The antitumor efficacy of adoptive T-cell therapy is dependent on potency, expansion, and persistence of transferred T cells.⁶ Current approaches to increase T-cell efficacy include a combination with cytokine treatment,⁷ T-cell-specific subset purification⁸ and genetic knockout of immune inhibitory molecules known as immune checkpoints⁹ among others.⁶

Here we aim to improve engineered TCR T-cell efficacy through a combination of two compounds targeting epigenetic regulation and post-translational modification (PTM).

The first compound in this combination regimen is the hypomethylating drug 5-Aza-2' deoxycytidine (5-Aza-2').¹⁰ Interestingly, 5-Aza-2' is suggested to also have immunotherapy-enhancing potential. 5-Aza-2' enhances transcription of granzyme B and perforin, upregulates MHC class I and intercellular adhesion molecule 1 (ICAM-1), driving CD8+T cell towards a heightened activation state.^{11 12} Furthermore, hypomethylating agents overcome transcriptional repression induced by DNA methylation, enabling transcription of tumor suppressor genes and enabling tumor-specific transcripts that encode for neoantigens or tumor-associated antigens enhancing immunotherapy potential.^{13 14}

The second compound we employ is the small molecule SUMO E1 inhibitor TAK981¹⁵ because the PTM SUMO inhibits antitumor immune responses, and blocking of SUMOylation increases CD8+T cell activation and augments antitumor responses predominantly via upregulation of type I interferon signaling.^{16–19} Furthermore, abolishment of SUMOylation enhances MHC class I antigen presentation and consequently efficacy of immunotherapy possibly as a result of increased interferon signaling.²⁰

We have previously shown that a combination of 5-Aza-2' and SUMOylation inhibitor TAK981 possesses synergistic anticancer potential. Inhibition of SUMOylation enhances the 5-Aza-2'-induced entrapment of DNA methyl transferase 1 (DNMT1), resulting in more DNA damage.²¹ We found recently that these drugs synergize to kill B-cell lymphoma in vitro and in vivo.²² Our previous study was conducted in immunodeficient mice and therefore only demonstrated the combined cytotoxic potential of these drugs.

In this study, we hypothesized that the immunomodulatory potential of subcytotoxic dosage of 5-Aza-2' combined with regular dosing of TAK981 could be employed to potentiate TCR therapy. We investigate the potentiating effect of TAK981-mediated inhibition of SUMOylation and hypomethylation via 5-Aza-2' on targeted TCR therapy against acute myeloid leukemia (AML) and multiple myeloma (MM). The first line of treatment for AML is often effective, however, relapses occur frequently and patients with relapsed or refractory AML have poor prognosis.²³ MM, the second-most frequent hematologic tumor is an incurable malignancy of the plasma cells, although several available treatments can provide remission and prolong survival.²⁴ Therefore, new therapies including TCR therapy are in high demand for both malignancies and need to be further improved. Here we employ a xenograft NSG mouse model for both AML and MM with TCR T cells.³ High dosing of 5-Aza-2' is currently used to treat AML, however toxicity and therapy resistance are often observed for single compound use.¹⁰ Here, we employ the immune modulatory potential of both drugs, potentially preventing drug resistance and overcoming major toxicity issues via the use of subcytotoxic dosage of 5-Aza-2' and altered treatment frequency. We found that the combination of drugs

strongly synergizes to potentiate TCR therapy, enabling effective eradication of AML and MM in vivo, by strong expansion of T cells, and optimization of T-cell tumor cell interaction.

MATERIALS AND METHODS

Materials and methods are described in detail in the online supplemental file.

RESULTS

Synergistic cytotoxic potential of SUMOylation inhibition and 5-Aza-2' to inhibit acute myeloid leukemia and multiple myeloma in vitro

First, we addressed the synergistic cytotoxic capacity of TAK981 and 5-Aza-2' on AML. TAK981 is a SUMOylation inhibitor, acting via blocking the SUMO E1 enzyme and consequently abrogating SUMOylation of target proteins (online supplemental figure 1A). 5-Aza-2' entraps DNMT1 to DNA, resulting in DNA-protein cross-links that block replication, leading to cytotoxic stress (figure 1A). Trapped DNMT1 needs to be SUMOylated to be degraded, providing the molecular basis for the synergistic cytotoxic potential of these drugs.^{21 22}

TAK981 inhibited conjugation of SUMOs to target proteins in AML and MM cell lines as expected and did not interfere with ubiquitylation, demonstrating specificity (online supplemental figure 1B, C). TAK981 and 5-Aza-2' individually inhibited AML and MM cell growth in vitro in a dose-dependent manner (figure 1B, C, online supplemental figure 1D, E). Combining low nanomolar dosage of TAK981 and 5-Aza-2' synergistically reduced tumor cell viability in AML in vitro (figure 1D and online supplemental figure 1F) consistent with current literature.²² To reduce viability in MM, a 10-fold higher dosage of TAK981 and 5-Aza-2' was required.

TAK981 and 5-Aza-2' synergize to potentiate NPM1-TCR activity in vivo

Following the strong synergistic effect of 5-Aza-2' and TAK981 in vitro, we continued to apply this strategy in vivo. For in vivo validation, 5-Aza-2' and TAK981 were combined with TCR therapy, following the strong evidence in recent literature that SUMO influences among others type I interferon signaling.^{16–18} We employed the previously established NPM1-TCR model, that contains a 4bp frameshift insertion within the NPM1 gene, resulting in a C-terminal alternative reading frame of 11 aa.³ This represents the most frequent AML subtype. Detailed on-target specificity of the HLA-A*02:01 restricted NPM1-TCR specific for mutant (m) NPM1 has been established previously.³ Immunocompromised NSG mice were engrafted with luciferase transduced OCI-AML3 cells (HLA-A*02:01+, mNPM1+) for 10 days, followed by two rounds of compound treatment and intravenous inoculation of NPM1-TCR or CMV-TCR CD8+T cells on day 15 (figure 2A). Compound

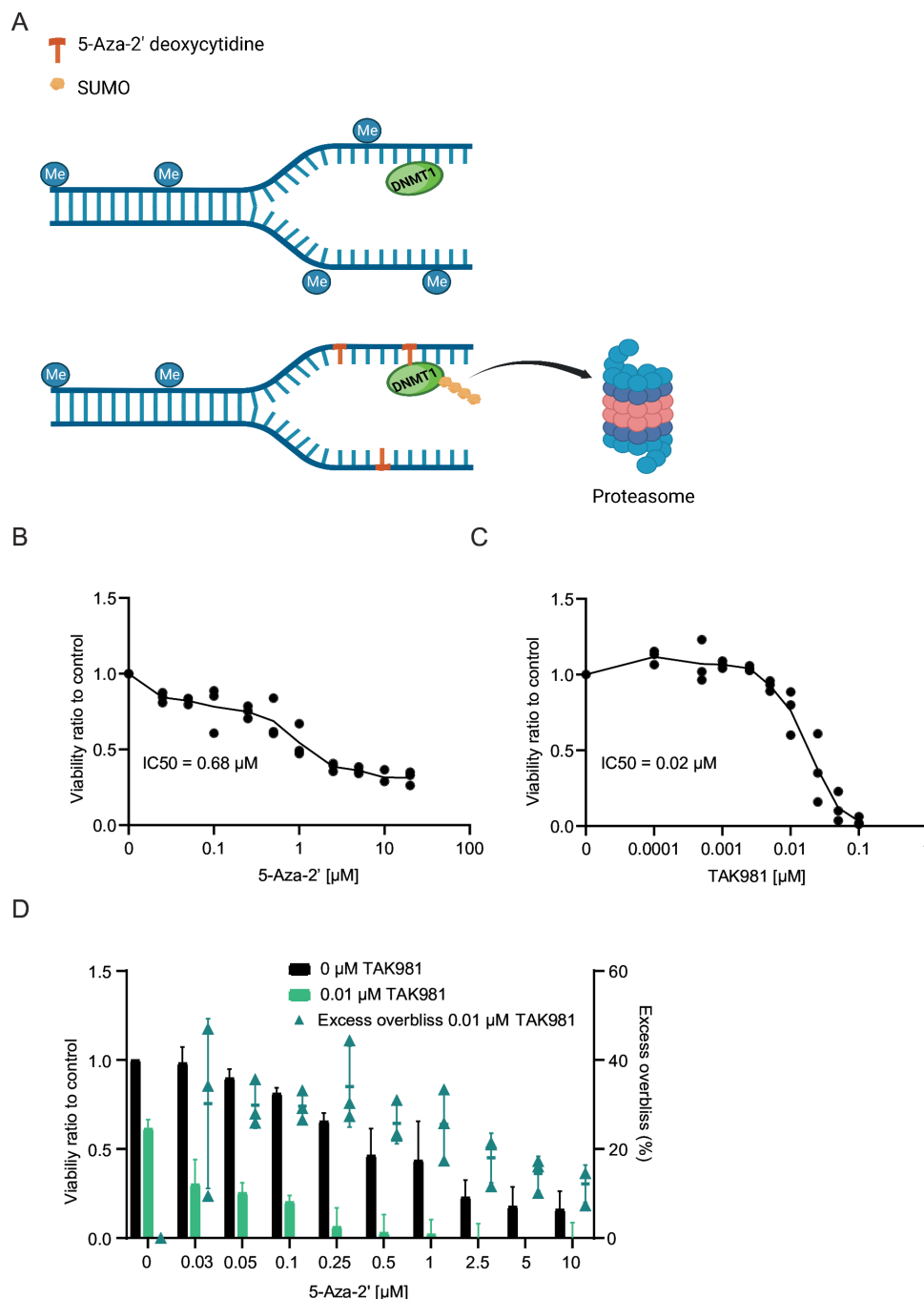


Figure 1 TAK981 and 5-Aza-2' synergistically reduce OCI-AML3 viability. (A) Mode of action of hypomethylation drug 5-Aza-2'-deoxycytidine. 5-Aza-2' incorporates into the DNA and entraps DNA methyl transferase 1 (DNMT1). Trapped DNMT1 is SUMOylated and degraded by the proteasome. (B) OCI-AML3 cell viability is shown after 4 days of 5-Aza-2' treatment (0.025–20 μ M) or control DMSO 0.01% treatment. IC₅₀ was calculated with GraphPad Prism V.9.3.1 (n=3). (C) OCI-AML3 cell viability after 4 days of TAK981 treatment (0.0001–0.1 μ M) or control DMSO 0.01% treatment. IC₅₀ was calculated with GraphPad Prism V.9.3.1 (n=3). (D) OCI-AML3 cell viability after 4 days of combination treatment with dose-response range of 5-Aza-2' combined with 10 nM of TAK981. Excess overbliss calculations of single 5-Aza-2' doses versus 5-Aza-2' doses with 10 nM TAK981 are provided to show drug synergy.

treatment was continued biweekly. NPM1-TCR therapy combined with 5-Aza-2' and TAK981 (“triple” therapy) demonstrated a striking better antitumor effect in the OCI-AML3 xenograft model compared with single and double treatments (figure 2B–D, online supplemental figure 2D). The reduction in tumor outgrowth obtained with the triple combination therapy was preserved for

over 40 days in half of the mice after cessation of the drug treatment (figure 2C). In contrast, single compound treatments did not significantly reduce OCI-AML3 tumor outgrowth (figure 2B, online supplemental figure 2A). TAK981 significantly potentiated NPM1-TCR therapy, whereas TAK981 treatment had no benefit over control therapy (figure 2D, online supplemental figure 2B). The

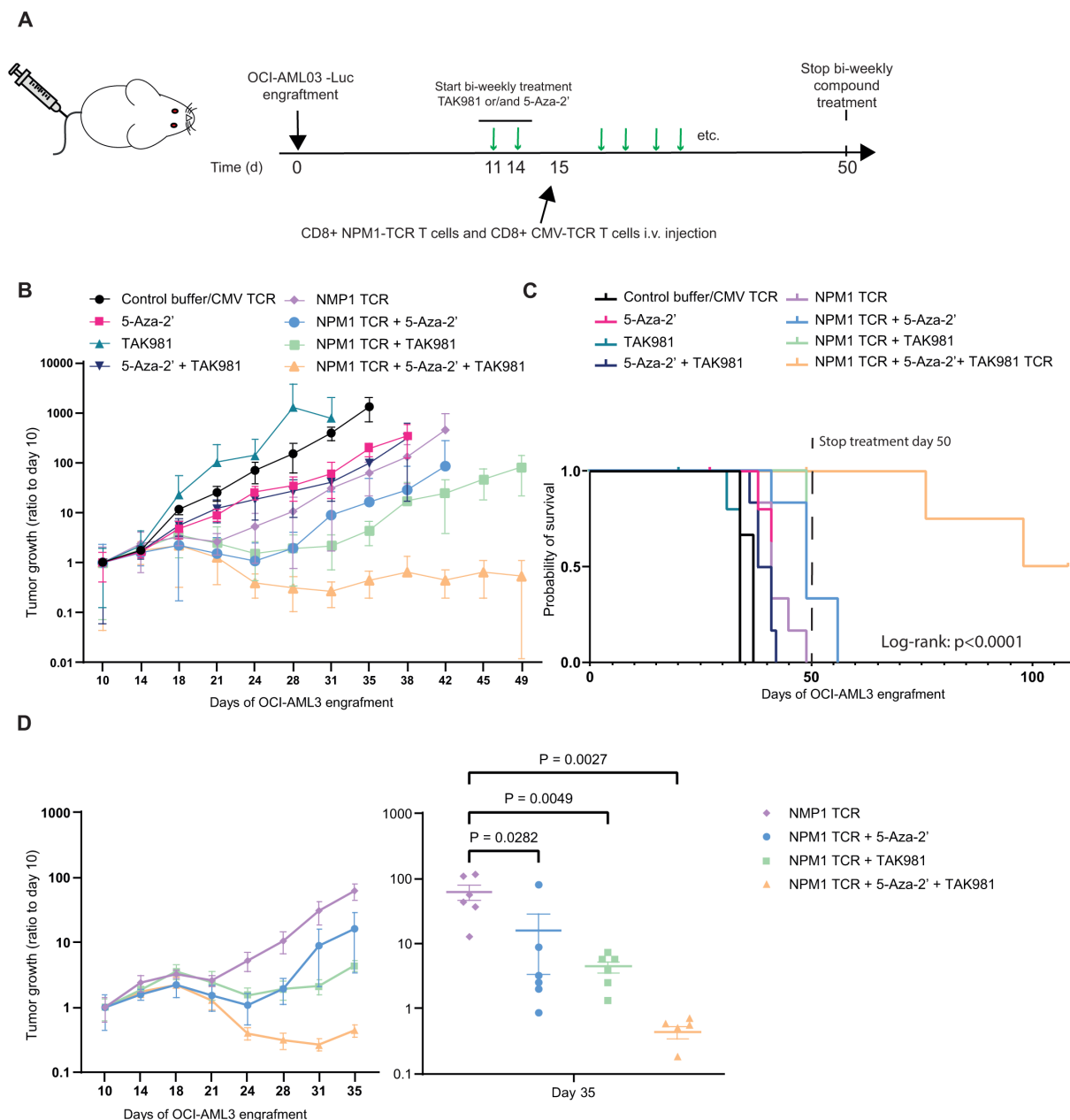


Figure 2 NPM1-TCR CD8+T cell antitumor efficacy is enhanced by 5-Aza-2' and TAK981 in vivo. (A) Timeline of in vivo experiment. Luciferase-expressing OCI-AML3 cells (1×10^6) were injected intravenously into the tail vein of NSG mice and engrafted for 10 days. Tumor volume was measured by IVIS. At day 10 treatment was started. Two rounds of the drug treatment with TAK981 (25 mg/kg) and/or 5-Aza-2' (2.5 mg/kg) were carried out. Subsequently, NPM1-TCR or CMV-TCR CD8+T cells (3×10^6) were intravenously injected on day 15. Biweekly drug treatments were continued until day 50 post-tumor injection. (B) OCI-AML3 tumor outgrowth average per group (n=6/7), control group consisted of 20% (2-hydroxypropyl)- β -cyclodextrin (HPBCD) buffer (n=3) and CD8+CMVTCR (n=3), which both fail to inhibit tumor outgrowth as shown in online supplemental figure 2E. Relative bioluminescent signal (BLI photons/sec/cm²/r) per mouse at day 10 is shown. (C) Survival curves for each group from B. The spaced line at day 50 indicates the end of the drug treatment. (D) Average OCI-AML3-Luc tumor outgrowth per group (n=6) ratio to bioluminescent (BLI photons/sec/cm²/r) signal per mouse at day 10. Graphs represent the time point when all mice were present in the experiment. A selection of groups from (B) containing at least NPM1-TCR as therapy are shown. One-way analysis of variance analysis was performed for tumor signals at day 35, in GraphPad Prism V.9.3.1. TCR, T-cell receptor.

combination of 5-Aza-2' with NPM1-TCR therapy was additive (figure 2D, online supplemental figure 2C). The prolonged tumor reduction with combination therapies suggests prolonged and/or heightened effectivity of the T cells in combination with 5-Aza-2' and TAK981.

To investigate whether the efficacy of the triple therapy was not restricted to the NPM1 specificity of the TCR, we repeated the experiment with a similar dosing regimen but with another antigen specificity of the TCR-modified CD8+T cells (online supplemental figure 2F). OCI-AML3

(HLA-A*02:01+HA2+) engrafted NSG mice were treated with a suboptimal dose of HA2-TCR CD8+T cells specific for the HA2 minor histocompatibility antigen in the context of HLA-A*02:01.²⁵ Treatment of OCI-AML3 engrafted NSG mice with the HA2-TCR CD8+T cells alone did not reduce OCI-AML3 outgrowth (online supplemental figure 2G). TAK981 alone could not potentiate the HA2-TCR T cells and 5-Aza-2' gave some reduction of the tumor outgrowth. In contrast, combining HA2-TCR therapy with both drugs showed a major reduction in OCI-AML3 outgrowth, underlining the efficacy of the triple therapy (online supplemental figure 2G).

To further strengthen our findings, we investigated whether the efficacy of the triple therapy was not restricted to AML but could be extended to other hematological malignancies. For this purpose, we employed an MM xenograft model with luciferase transduced U266 cells (HLA-A*02:01+, HLA-B*07:02+, BOB1+, MAGE-A1+) targeted by an HLA-B*07:02 restricted BOB1-TCR²⁶ or HLA-A*02:01 restricted MAGE-A1-TCR.⁵ Single compound treatment as well as a combination of both 5-Aza-2' and TAK981 had no effect on U266 outgrowth (online supplemental figure 3A), comparable to the poor effect on OCI-AML3 (figure 2B and online supplemental figure 2A). We then treated MM-engrafted NSG mice with suboptimal doses of BOB1-TCR or MAGE-A1-TCR T cells to investigate increased efficacy with TAK981 or 5-Aza-2', or both. Treatment with low numbers of BOB1-TCR T cells alone did not reduce U266 outgrowth. Combination with TAK981 alone could also not potentiate the TCR efficacy as a single compound. However, a combination of both drugs with TCR therapy caused clear tumor reduction (online supplemental figure 3B). Treatment with MAGE-A1-TCR T cells reduced U266 outgrowth in vivo. Additional treatment with TAK981 or 5-Aza-2' did potentiate the T-cell therapy (online supplemental figure 3C). Once more, the triple combination gave an even faster and larger reduction in tumor outgrowth compared with the dual combinations. These results demonstrate the strength of the triple therapy. Boosting TCR therapy with single compounds partially depends on the potential of TCR T cells towards the tumor. TAK981 can potentiate TCR therapy only when CD8+T cells show initial effectivity.

Immunomodulatory effect of TAK981 and 5-Aza-2' on CD8+ T cells

Next, we investigated the immunomodulatory properties of both drugs on the T cells in vitro. Activated CD8+T cells were treated overnight with low concentrations of TAK981 and/or 5-Aza-2', after which expression of different cytokine signaling and cytolytic pathways were measured. We measured interferon, interleukin and cytolytic molecule signaling at the transcriptional level via quantitative PCR analysis. Combining low doses of TAK981 (10 nM) and 5-Aza-2' (25 nM) increased transcription of both type I (IFN- α and IFN- β) and type II interferon (IFN- γ), IFN-stimulated genes and transcription factors, and

transcription of interleukins (figure 3A). 10-fold higher dosage of TAK981 single treatment induces transcription of IFN-related genes as expected (online supplemental figure 4A).^{17,18} We observed that 100 nM TAK981 (online supplemental figure 4A) resulted in substantially higher expression of IFN and IFN-related genes compared with 10 nM TAK981 (figure 3A). Furthermore, 10-fold higher dosage of 5-Aza-2' (250 nM) induces transcription of cytolytic molecule granzyme B.¹¹ A combination of a higher dosages of TAK981 and 5-Aza-2' did not lead to a proper readout due to cytotoxic effects (online supplemental figure 4D). We use subcytotoxic dosage of 5-Aza-2' for the combination treatment to realize induction of cytokine transcription (figure 3A).

Subsequently, we investigated whether TAK981 and 5-Aza-2' enhance the reactivity of NPM1-TCR CD8+T cells towards OCI-AML3 cells in vitro, since NPM1-TCR CD8+T cells recognize the mutated neoantigen NPM1 in the context of HLA-A*02:01 that are both expressed by OCI-AML3 cells.³ OCI-AML3 or NPM1-TCR CD8+T cells were pretreated for 4 days with 10 nM TAK981 and/or 25 nM 5-Aza-2' or DMSO 0.01% as control. Drug-treated OCI-AML3 or NPM1-TCR CD8+T cells were co-cultured with untreated NPM1-TCR CD8+T cells or OCI-AML3 cells overnight (figure 3B). Pretreatment of OCI-AML3 target cells did not lead to a significant increase in IFN- γ production (figure 3C), whereas pretreatment of NPM1-TCR CD8+T cells with TAK981 potentiated reactivity of T cells towards OCI-AML3 targets cells, IFN- γ production doubled compared with DMSO control (figure 3D, online supplemental figure 4B). Combining pretreated NPM1-TCR CD8+T cells and pretreated OCI-AML3 cells showed that mainly SUMOylation inhibition is responsible for the induction of IFN- γ in vitro (online supplemental figure 4E, F). Taken together, our data show that subcytotoxic dosage of 5-Aza-2' combined with the regular dosage of TAK981 has immunomodulatory capacity towards CD8+T cells.

TAK981 and 5-Aza-2' synergize to induce CD8+ T-cell proliferation in vivo

Based on the observation that combination treatment enhanced the in vivo responses induced by TCR T cells, we hypothesized that combination treatment might affect T-cell activation state and/or persistence. To gain insight into the effect of TAK981 and 5-Aza-2' on NPM1-TCR CD8+T cell proliferation and persistence in vivo, we generated luciferase expressing CD8+T cells. This approach allowed us to locate and quantify NPM1-TCR CD8+T cells in mice, using a similar experimental setting as presented in figure 3. NSG mice were transplanted with OCI-AML3 (non-luciferase) cells, treated on days 14 and 17 with the two drugs and subsequently inoculated with NPM1-TCR CD8+LucT cells at day 18. Drug treatment was continued biweekly as indicated. Bioluminescence of NPM1-TCR T cells was measured on days 3, 6 and 9 post T-cell injection (figure 4A). Strikingly, combining 5-Aza-2' and TAK981 treatment led to a 10-fold higher BLI signal

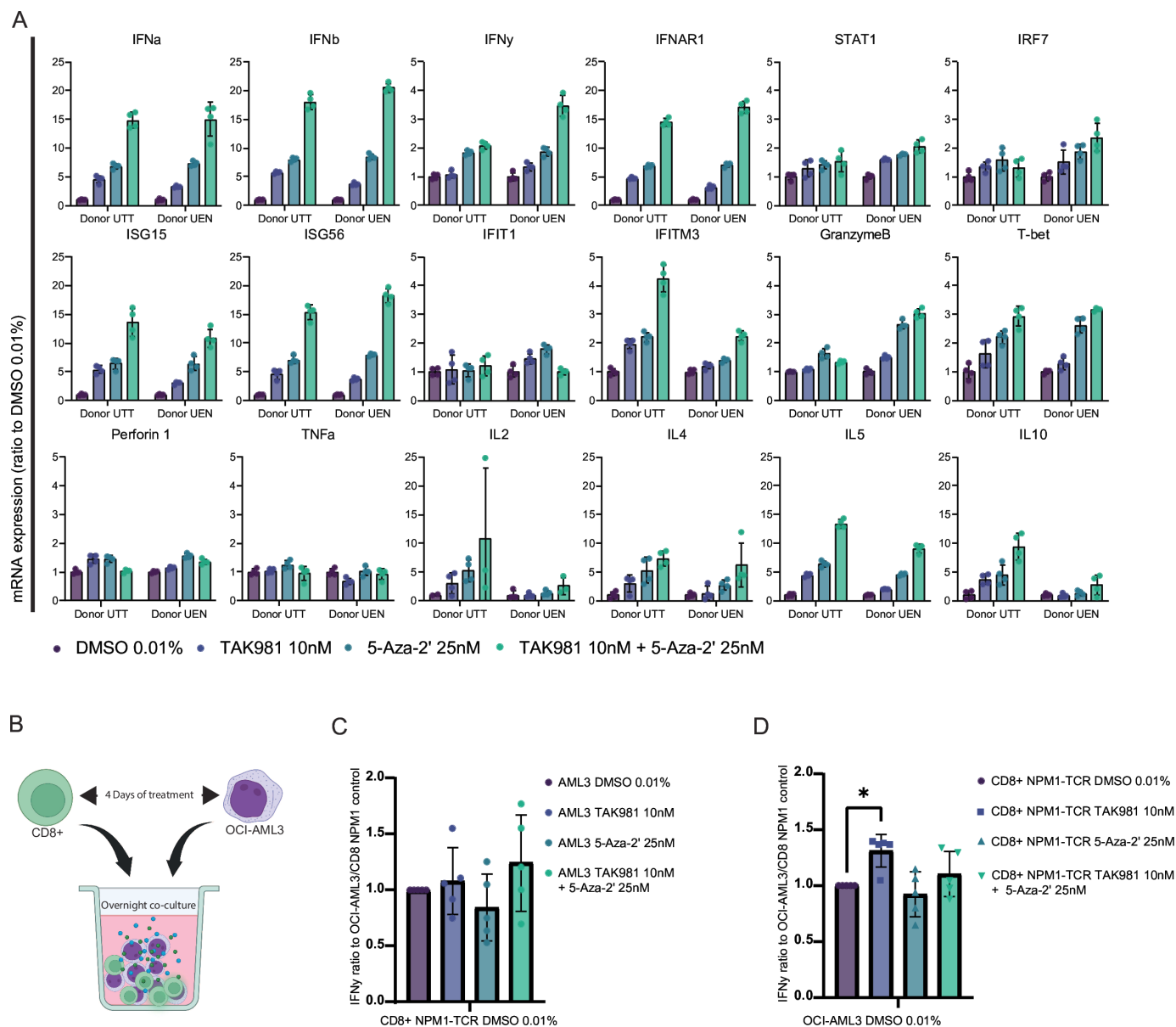


Figure 3 SUMOylation inhibition in combination with hypomethylation activates the interferon pathway, cytokine production and cytolytic compound signaling in CD8+T cells. (A) CD8+T cells were isolated from three different healthy donors. CD8+ were treated 10 days post stimulation with 10nM TAK981 and/or 25nM 5-Aza-2' or DMSO 0.01% as control overnight. mRNA expression levels of IFN- γ , IFN- β , IFN- α , STAT1, IFNAR1, IFIT1, IFITM3, ISG15, ISG56, IRF7, T-bet, TNF- α , granzyme B, perforin-1, IL-2, IL-4, IL-5 and IL-10 were measured using quantitative PCR. 18sRNA, SDHA and SRPR were used as housekeeping genes. Expression was plotted as a ratio to DMSO 0.01% control, individual per donor (n=3). *p<0.05, **p<0.01, ***p<0.001, two-way ANOVA compared with DMSO 0.01%, followed by Dunnett multiple comparison correction GraphPad Prism V.9.3.1. (B) Experimental co-culture set-up to measure the production of IFN- γ by CD8+T cell on co-culture with OCI-AML3 target cells. Either CD8+T cells or OCI-AML3 cell were pretreated with TAK981 and/or 5-Aza-2' pre-overnight co-culture. (C) OCI-AML3 target cells were pretreated on days 4 and 1 with 10nM TAK981 and/or 25nM 5-Aza-2'. Subsequently, OCI-AML3 cells were co-cultured overnight with CD8+T cells. Supernatant was harvested and analyzed by IFN- γ ELISA. Five different donors were used for the generation of CD8+NPM1 TCR T cells. *p<0.05, two-way ANOVA compared with DMSO 0.01%, followed by Fisher's LSD test, GraphPad Prism V.9.3.1. (D) CD8+T cells were pretreated on days 4 and 1 with 10nM TAK981 and/or 25nM 5-Aza-2'. Subsequently, CD8+T cells were co-cultured with OCI-AML3 cells overnight. Supernatant was harvested and analyzed by IFN- γ ELISA. Five different donors were used for the generation of CD8+NPM1 TCR T cells *p<0.05, two-way ANOVA compared with DMSO 0.01%, followed by Fisher's least significant difference test, GraphPad Prism V.9.3.1. ANOVA, analysis of variance; IFN, interferon; mRNA, messenger RNA; TCR, T-cell receptor.

at day 6 compared with the single T-cell treatment or double combinations (figure 4B and C). This correlated with elevated numbers of CD8+T cells harvested from the

bone marrow of triple-treated mice (figure 4D). TAK981 treatment induced a modest increase in NPM1-TCR T cells on days 6 and 9. 5-Aza-2' treatment boosted

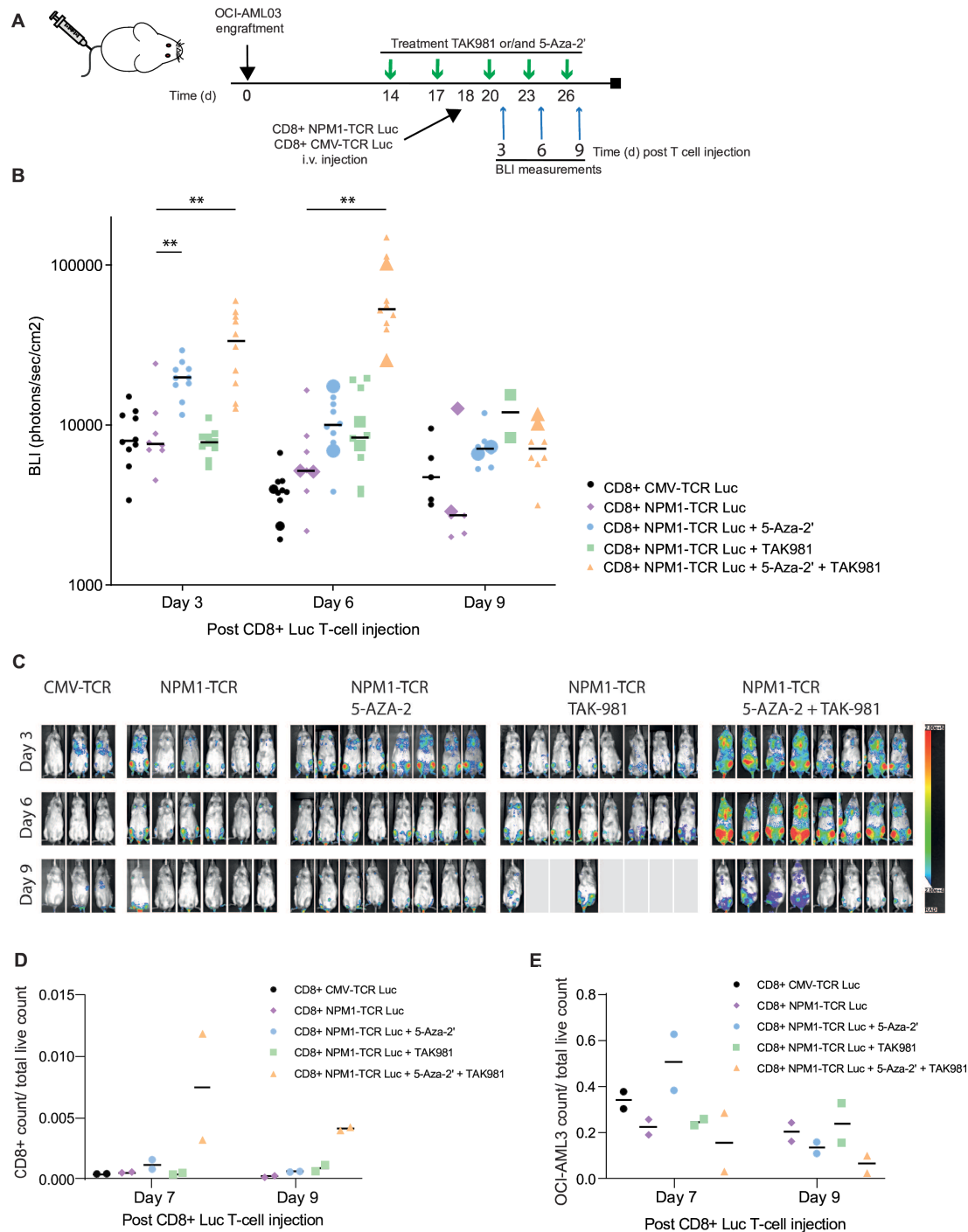


Figure 4 Combination therapy of 5-Aza-2' and TAK981 potentiates CD8+T cell proliferation in vivo. (A) Time line of in vivo experiment. Luciferase expressing NPM1-TCR or CMV-TCR CD8+T cells (3×10^6) were injected 18 days post OCI-AML3 (1×10^6) engraftment. Two times dosing with TAK981 (25 mg/kg) and/or 5-Aza-2' (2.5 mg/kg) prior to T-cell injection was performed and three times following T-cell injection, matching the dosing time to figure 3. Bioluminescence (photons/sec/cm²/r) was measured at indicated time points on days 3, 6 and 9 post T-cell injection. (B) Raw values of ventral BLI signal (photons/sec/cm²/r) for days 3, 6 and 9 are visualized per group. Each dot represents an individual mouse. Differences to CD8+NPM1 TCR Luc group were analyzed per time point via two-way analysis of variance (mixed model) followed by Tukey multiple comparisons. * $p < 0.05$, ** $p < 0.01$ (day 3: $n = 10$ per group, day 6: $n = 8$ per group) (C) Visualization of luciferase transduced CD8+T in all mice imaged in figure 4B. Scaling for bioluminescence was kept the same for each time point (Living Image Software). Six mice in the NPM1-TCR/TAK981 group reached the humane endpoint. (D) Ratio of CD8+ cells per total live cells (human and mouse) in bone marrow. (E) Ratio of OCI-AML3 cells per total live cells (human and mouse) in bone marrow. Samples were taken from mice depicted in figure 4B, large symbols for mice on day 6 match the ratio OCI-AML3+counts/total live count for day 7 and large symbols for mice on day 9 match the ratio OCI-AML3+counts/total live count for day 9. Day 9 samples containing CD8+CMV TCR T cells were not included due to lack of live cells (online supplemental figure 5). Gating strategy is shown in online supplemental figure 5A. B. i.v., intravenously; TCR, T-cell receptor.

NPM1-TCR T cells at an early stage; however, this boost was reduced on day 6. On day 9 BLI signal decreased again for the NPM1-TCR T cells treated with 5-Aza-2' and TAK981, whereas total CD8+T cell count from the bone marrow showed persistent elevation (figure 4D). Furthermore, measuring the total OCI-AML3 counts within the harvested bone marrow samples confirmed the efficiency of the triple therapy (figure 4E).

TAK981 and 5-Aza-2' synergize to increase in vivo activity of NPM1-TCR CD8+ T cells

To gain more insight into the mechanisms underlying the efficacy of the triple therapy, we conducted spectral flow cytometry analysis on the bone marrow of OCI-AML3 engrafted NSG-mice at several days after NPM1-TCR T-cell injection and compound treatment (figure 5A). On days 2, 5 and 8 post NPM1-TCR T-cell injection, bone marrow was harvested and spectral flow cytometry analysis was performed both on the NPM1-TCR CD8+T cells (figure 5) and OCI-AML3 cells (figure 6). Consistent with figure 4 the total T-cell counts were highest at day 5 and day 8 in the group treated with the combination of 5-Aza-2' and TAK981 (figure 5B). In line with this finding, the increase of Ki67-positive cells was also most pronounced in mice treated with the combination of 5-Aza-2' and TAK981, up to approximately 60% of the T cells were positive for Ki67 in this group. In general, the percentage of T cells expressing the proliferation marker Ki67 increased in all treatment groups at day 5 after infusion, indicating antitumor activity. An increase of approximately 20% was shown for mice treated with TAK981 or no drug treatment and approximately 40% for 5-Aza-2' treated mice (figure 5C). In all groups, the percentage of T cells expressing Ki67 dropped at day 8, however in the triple treatment group the level of Ki67 expression on TCR T cells was still increased compared with day 2. Together these findings demonstrate that the combination of 5-Aza-2' and TAK981 leads to strong in vivo proliferation of transferred tumor targeting TCR T cells.

Furthermore, the percentage of interferon transcription factor 1 (IRF1) positive T cells in mice treated with 5-Aza-2' and TAK981 was dramatically increased and sustained compared with control or single drug treatment. The 5-Aza-2' single-treatment equally increased the percentage of IRF1 positive T cells at day 2, however, this effect did not persist to later time points (figure 5C).

Interestingly, the NPM1-TCR T cells in triple-treated mice showed no increase in early activation/differentiation markers such as ICOS, CD137, CD25, PD-1, and LAG3 compared with no or single-drug-treated mice (figure 5C). NPM1-TCR T cells in 5-Aza-2' or TAK981 treatment conditions showed increased expression of activation markers ICOS, PD-1, LAG3 and CD137. For 5-Aza-2' treatment, the expression peaked on day 5, whereas for TAK981 treatment

most activation markers increased till day 8, which corresponds with the hypothesis that TAK981 facilitates prolonged T-cell activation and persistence, and therefore prolonged repression of tumor outgrowth as presented in figure 2. In contrast, we show that HLA-DR was typically upregulated for a prolonged time in the NPM1-TCR T cells of all treatment groups. In the triple therapy group, HLA-DR was the earliest and highest upregulated, correlating with the largest activation response. Taken together, triple therapy leads to upregulation of Ki67, IRF1 and HLA-DR, whereas early activation and differentiation markers were not increased.

TAK981 and 5-Aza-2' increase immunogenicity of tumor cells

Antigen presentation by HLA class I molecules is vital for CD8+T cell recognition of tumor cells. To investigate whether 5-Aza-2', TAK981 or a combination of treatment potentiates the T-cell reactivity via changes in HLA class I expression as well as adhesion and co-inhibitory or co-stimulatory molecules, we analyzed OCI-AML3 tumor cells from the bone marrow of NSG mice by spectral flow cytometry. Bone marrow was harvested 18 days post engraftment after three rounds of treatment (figure 6A). Tumor cell surface molecules involved in the interaction between T cell and tumor cell were investigated (figure 6B). TAK981 and 5-Aza-2' single or combination treatments all induced upregulation of HLA class I and co-stimulatory ligand CD86, which was most prominent in the triple treatment. Adhesion molecules CD54 and CD58 were not changed or slightly downregulated on the different treatments. Interestingly, programmed cell death 1 ligand 1 (PD-L1) a key immune checkpoint facilitating immune escape, was downregulated on 5-Aza-2' single treatment and even more pronounced in combination with TAK981 (figure 6B).

Subsequently, we investigated whether the interaction with the TCR CD8+T cells would influence HLA class I molecule and PD-L1 expression on OCI-AML3 cells. Mice were drug treated two times prior to T-cell injection, and on days 2, 5 and 8 post NPM1-TCR T-cell injection, bone marrow was harvested and spectral flow cytometry analysis was performed on the OCI-AML3 cells (figure 6C). At day 2 after T-cell infusion the expression of HLA class I, ki67 and PD-L1 on the OCI-AML3 (figure 6D) resemble the expression as measured without infusion of the T cells (figure 6B). HLA class I upregulation at day 2 was most prominently observed for the triple treatment, and PD-L1 downregulation was also most prominently observed in the triple therapy (figure 6D). Treatment with 5-Aza-2' in the presence of T cells also resulted in an increase in ki67 in the OCI-AML3 tumor cells. At day 5 after T-cell infusion HLA class I cell surface expression on the OCI-AML3 was further upregulated in the presence of NPM1-TCR T cells treated in vivo with TAK981 (figure 6D). Due to treatment efficiency, no OCI-AML3 cells were left for analysis in the triple combination group on days 5 and 8 after T-cell infusion. In accordance, single-cell gene

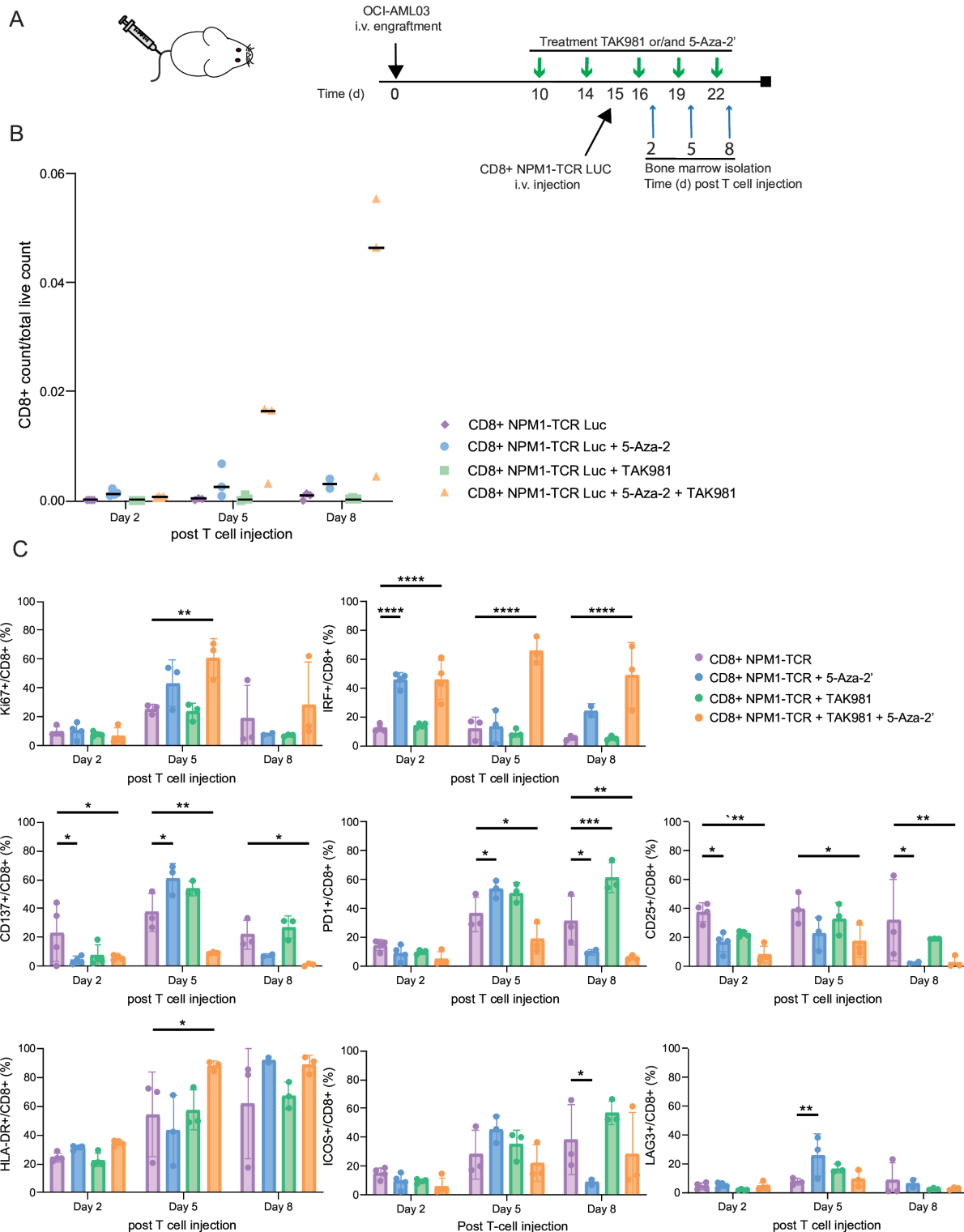


Figure 5 SUMOylation inhibition enhances NPM1-TCR CD8+T cell activation and in combination with 5-Aza-2' increases proliferation in vivo. (A) Timeline of in vivo experiment; NSG-mice were engrafted with OCI-AML3 cells for 14 days followed by treatment with 25 mg/kg TAK981 and/or 2.5 mg/kg 5-Aza-2' or with a buffer control on the indicated days. NPM1-TCR CD8+T cells were injected on day 15 post OCI-AML3 engraftment. Harvesting of bone marrow occurred on days 2, 5 or 8 post inoculation with the NPM1-TCR CD8+Luc T cells and analyzed with spectral flow cytometry. n=4 per group for day 2, n=3 per group for day 5 and 8. (B) Ratio of CD8+count/total live (human and mouse) count in bone marrow. Samples were used for marker analysis (figure 5C) of CD8+NPM1 TCR Luc T cells and OCI-AML3 cells. (C) Bar-graphs represents the percentage of Ki67, IRF1, CD137, PD-1, CD25, HLA-DR, ICOS and LAG3 positive NPM1-TCR CD8+T cells from bone marrow as described in figure 5A. Differences between control (CD8+NPM1 TCR) and treated groups per day were calculated via two-way analysis of variance followed by Dunnett multiple comparison *p<0.05, **p<0.01, ***p<0.001, ****p<0.0001. i.v., intravenously; TCR, T-cell receptor.

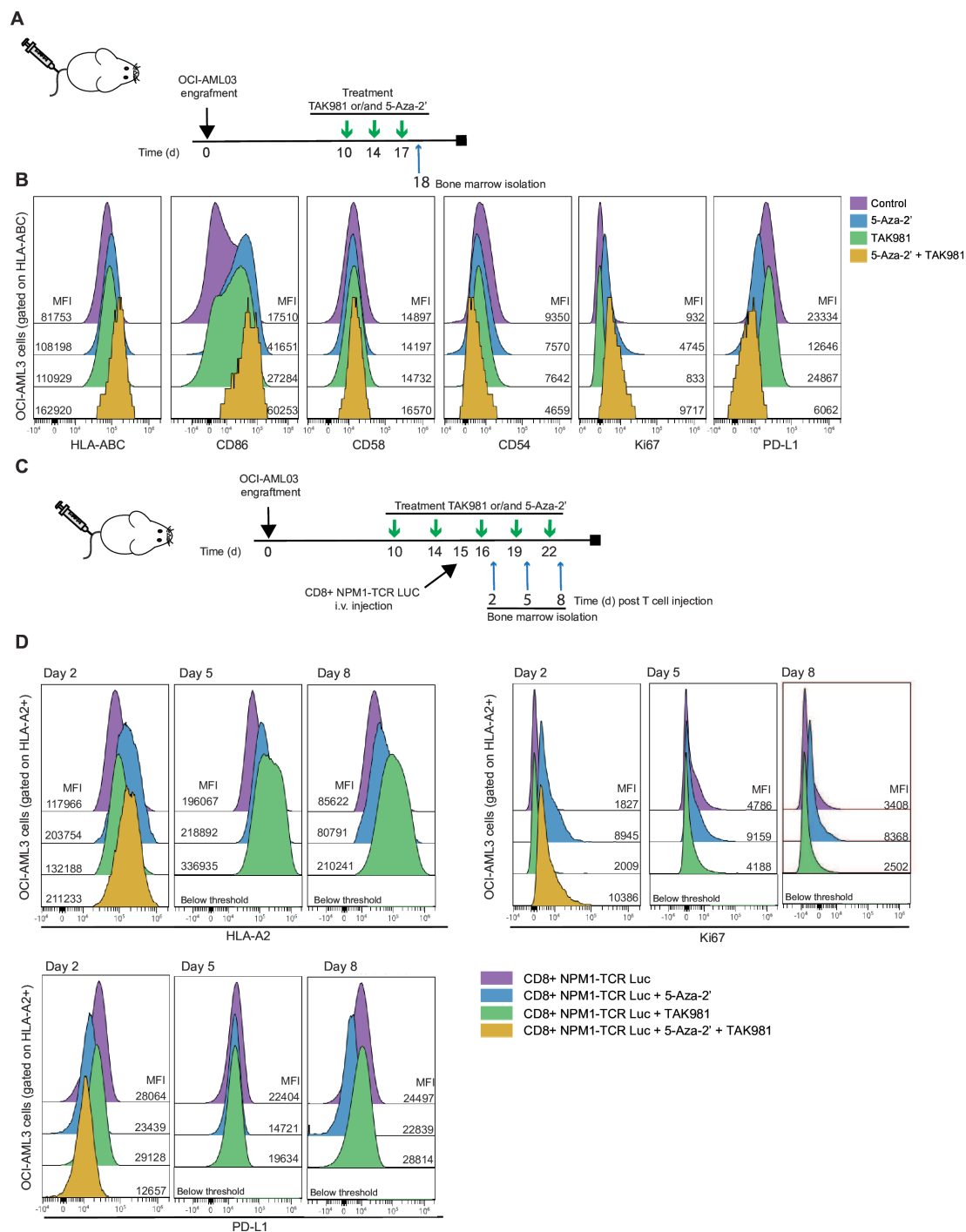


Figure 6 SUMOylation inhibition and 5-Aza-2' improve immunogenicity of tumor cells. (A) Timeline of in vivo experiment; NSG-mice were engrafted with OCI-AML3 cells for 10 days followed by treatment with 25 mg/kg TAK981 and/or 2.5 mg/kg 5-Aza-2' or with a buffer control on the indicated days. Consequently, bone marrow was harvested on day 18 and analyzed with spectral flow cytometry. (B) Histogram plots show marker expression of HLA-ABC, CD86, CD58, CD54, Ki67 and PD-L1 on OCI-AML3 cells. Plots include the average MFI signal per group. Control (n=4), 5-Aza-2' (n=4), TAK981 (n=4), TAK981 and 5-Aza-2' (n=2). Samples were removed from analysis if insufficient OCI-AML3 cells were present total count <1000. Gating strategy is shown in online supplemental figure 6. (C) Timeline of in vivo experiment; OCI-AML3 cells were engrafted for 10 days in NSG-mice. Mice were treated with 25 mg/kg TAK981 and/or 2.5 mg/kg 5-Aza-2' or with a buffer control on indicated days. NPM1-TCR CD8+T cells were injected on day 15 post OCI-AML3 engraftment. OCI-AML3 cells were analyzed from bone marrow harvested on days 2, 5 or 8 post injection with the NPM1-TCR CD8+Luc T cells via spectral flow cytometry. (D) Histogram plots show marker expression of HLA-A2, Ki67 and programmed cell death 1 ligand 1 (PD-L1) on OCI-AML3 cells from mice also inoculated with NPM1-TCR CD8+T cells. Plots include the average Mean Fluorescence Intensity (MFI) signal per group. Samples were removed from analysis if insufficient OCI-AML3 cells were present in sample, indicating a total count of cells <300 for day 2 samples and <1000 for day 5 and 8 samples. Gating strategy is shown in online supplemental figure 6. i.v., intravenously; TCR, T-cell receptor.

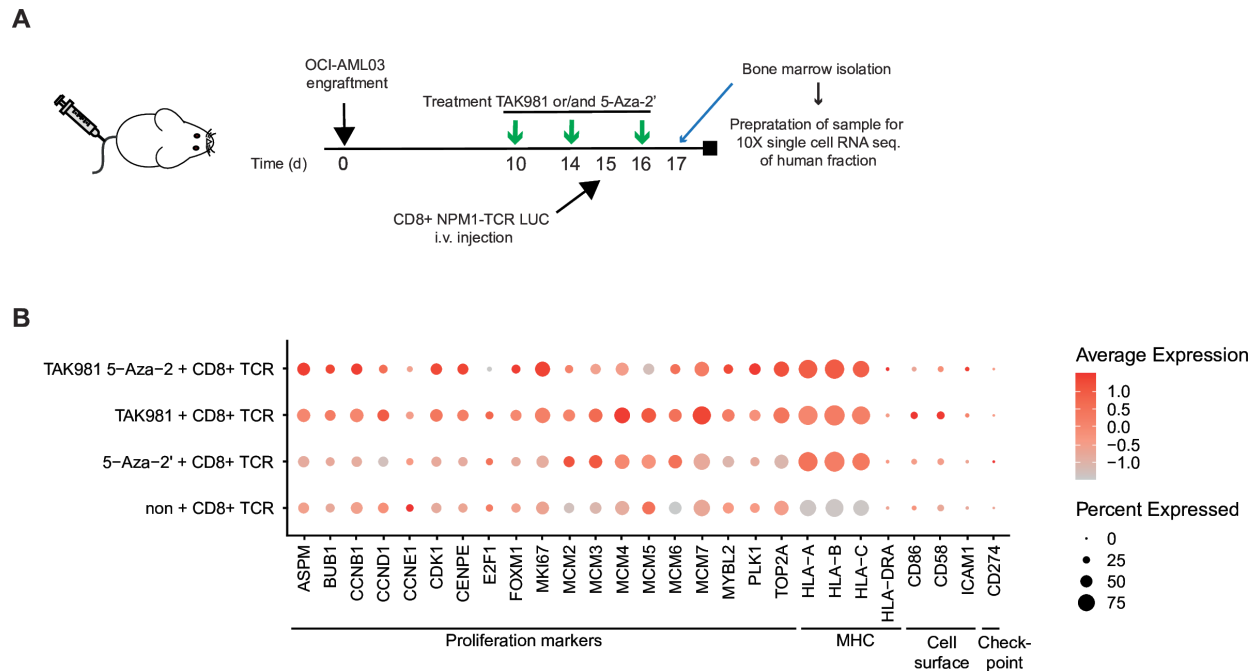


Figure 7 Single-cell sequencing of OCI-AML3 tumor cells from OCI-AML3 xenograft model. (A) Timeline of in vivo experiment; OCI-AML3 cells were engrafted for 10 days in NSG-mice. Mice were treated with 25 mg/kg TAK981 and/or 2.5 mg/kg 5-Aza-2' or with a buffer control on indicated days. NPM1-TCR CD8+T cells were injected on day 15 post OCI-AML3 engraftment. OCI-AML3 cells were harvested from bone marrow 2 days post injection with the NPM1-TCR CD8+Luc T cells and sent for single-cell sequencing. (B) Expression dotplot of single-cell sequencing data obtained from mouse bone marrow implanted with OCI-AML3 cells following treatments indicated in A. Genes for proliferation, MHC expression, cell surface and checkpoint are displayed. i.v., intravenously; MHC, major histocompatibility complex; RNA-seq, RNA sequencing; TCR, T-cell receptor.

expression analysis of tumor cells OCI-AML3 xenografts treated with NPM1-TCR T cells in the presence or absence of 5-Aza-2' and/or TAK981 (figure 7A) also indicated additional upregulation of MHC molecules in treatment groups (figure 7B). Furthermore, a cluster of proliferative markers was found to be upregulated in the OCI-AML3 cells in the triple therapy group.²⁷

Taken together, 5-Aza-2' and TAK981 regulate the expression of multiple different cell surface molecules thereby increasing the immunogenicity of tumor cells. Combined, these results provide insight into the potential molecular mechanism underlying the improved efficacy of TCR therapy by 5-Aza-2' and TAK981.

DISCUSSION

In this study, we evaluated a novel drug combination to augment TCR T-cell therapy. Excitingly, combining TCR T-cell therapy with the SUMO E1 inhibitor TAK981 and the DNA methylation inhibitor 5-Aza-2' resulted in strong antitumor activity against two in vivo tumor models of hematological malignancies using four engineered TCR T-cell specificities. We uncovered that the drug combination caused strong TCR T-cell proliferation in vivo. In addition, the drug combination increased cytokine signaling in T cells, and reduced differentiation towards exhausted phenotype, while simultaneously increasing the immunogenicity of the tumor by increasing HLA and co-stimulation but lowering inhibitory ligand expression.

Sustained cytokine signaling, ongoing proliferation, and reduced exhaustion of tumor-targeting T cells is a unique signature of this therapy. The proliferation of T cells and active IFN signaling are thought to be mutually exclusive because of the antiproliferative effect of IFN,²⁸ however, the drug combination induced a more than 10-fold increase in luciferase signal and CD8+T cell numbers at the peak of the antitumor immune response in vivo.

Both compounds contribute distinctively to the therapy efficacy. SUMOylation is known to block IFN transcription^{29,30}; consequently, SUMOylation inhibition by TAK981 enhances cytokine production in T cells. This is consistent with recent findings that TAK981 enhances T-cell IFN transcription and production,¹⁷⁻¹⁹ providing a mechanistic explanation for the positive effect of TAK981 on CD8+T cell activation in vivo. TAK981 efficacy is fully dependent on the presence of T cells, since single compound TAK981 treatment did not block tumor growth. Ex vivo evaluation of T-cell phenotype showed reduced upregulation of early and late activation markers over time, with the exception of HLA-DR, resulting in reduced differentiation towards the exhausted phenotype of T cells. Hypomethylation via 5-Aza-2' treatment results in additional removal of transcriptional blockage resulting in increased cytolytic compound production and in combination with TAK981 overall increase cytokine signaling.

Furthermore, induction of MHC I cell surface expression is observed on treatment of OCI-AML3 with 5-Aza-2' and TAK981 in the absence of T cells, whereas single treatment only marginally increased MHC I. In contrast, in the presence of T cells a large increase in MHC I cell surface expression was observed in an early response to 5-Aza-2' 2 days post T cells, whereas MHC I cell surface expression peaked 5 days after T-cell injection in response to TAK981 treatment. This is compatible with a slower but prolonged activation of TAK981 treatment compared with 5-Aza-2', and suggests that IFN production by T cells strongly contributes to MHC I upregulation on tumor cells. Our data on MHC I regulation corresponds with recent literature,²⁰ where it has been shown that active SUMO has repressive effects on MHC I cell surface expression. In addition, it was found previously that hypomethylation of antigen presentation complex (APC)-related genes by 5-Aza-2' enhanced antigen presentation on tumor cells.^{12, 31} Increased expression of APC machinery is not restricted to the MHC molecules but extends to CD86 co-stimulatory ligand. It has to be noted that CD54 was not upregulated in our ex vivo analysis after either 5-Aza-2' or TAK981 single treatment, in contrast to literature.¹² Interestingly, PD-L1 inhibitory ligand was downregulated early after 5-Aza-2' treatment, and combined drug treatment even downregulated PD-L1 expression more drastically, potentially reducing immune checkpoint signaling. This is in contrast with literature where 5-Aza-2' treatment upregulated PD-L1 expression,^{32, 33} which potentially could be explained by differences in dosage. Combined, these drugs mutually support the increased tumor-targeting potential of TCR therapy. Our data suggest that the "triple therapy" supports effective antitumor activity in a persistent manner, and reduces T-cell overactivation and differentiation towards exhausted phenotype. SUMO is reported to play a role in inducing exhaustion via aryl hydrocarbon receptor stability, whereas inhibition of SUMO leads to degradation of the aryl hydrocarbon receptor and consequently a decrease in exhaustion via this protein.³⁴ Naturally, T-cell exhaustion is a complex process,³⁵ and further research has to establish the full scale of mechanisms involved regarding T-cell immune responses and comprehend in vivo consequences of 5-Aza-2' and TAK981 treatment, in a dosage and cancer type-specific manner.

To fully understand the mechanisms underlying triple therapy efficacy, more research has to be conducted. Molecular understanding of the combinatorial efficacy of both compounds on TCR T-cell persistence, proliferation and activation and on tumor immunogenicity will be essential to further develop this therapeutic strategy. Extending the single-cell RNA sequencing with T cells harvested from the bone marrow was not successful. T-cell yield was very low, resulting in an insufficient number of T cells for proper single-cell analysis. Future efforts improving this technique would help in deep understanding of the pathways at play, extending our knowledge beyond the marker analysis for T cells and tumor cells presented here. In addition,

investigating the epigenetic profile of T cells on TAK981 and 5-Aza-2' treatment would create more insight in among others T-cell exhaustion mechanisms. SUMOylation and methylation are both important players in the regulation of gene transcription and therefore TAK981 and 5-Aza-2' are interesting epigenetic modulation compounds.

Furthermore, it is important to study the most optimal dosing regimen of the three components of the triple therapy. 5-Aza-2' and TAK981 display distinct functions within our therapy. It would be worthwhile to investigate pretreating the tumor with 5-Aza-2' only, or employing single 5-Aza-2' drug treatment post TCR T-cell injection once, followed by continuous treatment with TAK981. This strategy might limit the toxicity of 5-Aza-2' on rapidly proliferating T cells, while prolonged TAK981 treatment might still enhance the persistence of the TCR T cells.

Here, we already show the effectiveness of the triple therapy for two tumor types, each targeted by two different TCR T cells. Future research should address to what extent our findings can be extended to other target specificities and malignancies. It is especially challenging to treat solid "cold" tumors that are often less susceptible to T-cell therapy. Enhancement of T-cell proliferation and persistence and increasing the immunogenicity of the tumors are important features that might enable overcoming immunosuppressive tumor microenvironments.^{1, 36}

We provide evidence for a novel strategy to enhance TCR therapy with subcytotoxic dosing of 5-Aza-2' and regular dosing of TAK981. In summary, SUMOylation inhibition via TAK981 in combination with 5-Aza-2' synergizes to enhance cellular immunotherapy by altering transcriptional regulation of CD8+T cells, increasing cytokine production including IFNs indicating increased activation, whereas the differentiation towards an exhausted phenotype is reduced. Moreover, the immunogenicity of tumor cells is markedly increased. Combining TCR T-cell therapy with TAK981 and 5-Aza-2' represents an important step towards improved clinical outcome.

Author affiliations

¹Department of Cell and Chemical Biology, Leiden University Medical Centre, Leiden, The Netherlands

²Department of Hematology, Leiden University Medical Centre, Leiden, The Netherlands

³Department of Pathology, Leiden University Medical Centre, Leiden, The Netherlands

Contributors JSK, ACOV and MHMH conceptualized the project. JSK, ACOV and MHMH designed the experiments. JSK and AKW carried out in vitro experimental work. MG contributed the AML TCR model. TLAW and AFAST contributed to the in vitro experimental work. JSK, SK, DFGR, AKW, IJdG and TLAW carried out and contributed to in vivo experimental work. JPR and NFCCdM analyzed single-cell sequencing data. JSK analyzed all data. JSK drafted the manuscript. JSK, ACOV and MHMH edited the manuscript. ACOV and MHMH are guarantors of the study.

Funding This work was funded by the Dutch Cancer Society (grant 10835).

Competing interests LUMC has applied for a patent on the triple therapy with MHMH and ACOV as inventors.

Patient consent for publication Not applicable.

Ethics approval In vivo studies performed were approved by the national Ethical Committee for Animal Research (AVD116002017891).

Provenance and peer review Not commissioned; externally peer reviewed.

Data availability statement Data are available in a public, open access repository. The high throughput RNA sequencing data set is available in the Gene Expression Omnibus (GEO) from NCBI with accession number GSE267689.

Supplemental material This content has been supplied by the author(s). It has not been vetted by BMJ Publishing Group Limited (BMJ) and may not have been peer-reviewed. Any opinions or recommendations discussed are solely those of the author(s) and are not endorsed by BMJ. BMJ disclaims all liability and responsibility arising from any reliance placed on the content. Where the content includes any translated material, BMJ does not warrant the accuracy and reliability of the translations (including but not limited to local regulations, clinical guidelines, terminology, drug names and drug dosages), and is not responsible for any error and/or omissions arising from translation and adaptation or otherwise.

Open access This is an open access article distributed in accordance with the Creative Commons Attribution Non Commercial (CC BY-NC 4.0) license, which permits others to distribute, remix, adapt, build upon this work non-commercially, and license their derivative works on different terms, provided the original work is properly cited, appropriate credit is given, any changes made indicated, and the use is non-commercial. See <http://creativecommons.org/licenses/by-nc/4.0/>.

Author note During the revision of our work, a related paper was published by Gabellier et al. 2024 Haematologica. 109:98-114. doi: 10.3324/haematol.2023.282704, showing synergy between TAK981 and 5-azacytidine in preclinical models of AML.

ORCID iDs

Jessie S Kroonen <http://orcid.org/0000-0002-0997-6267>
Tassilo L A Wachsmann <http://orcid.org/0000-0001-9507-2530>
Noel F C C de Miranda <http://orcid.org/0000-0001-6122-1024>
Mirjam H M Heemskerk <http://orcid.org/0000-0001-6320-9133>
Alfred C O Vertegaal <http://orcid.org/0000-0002-7989-0493>

REFERENCES

- 1 Shafer P, Kelly LM, Hoyos V. Cancer therapy with TCR-engineered T cells: current strategies, challenges, and prospects. *Front Immunol* 2022;13:835762.
- 2 Sun Y, Li F, Sonnemann H, et al. Evolution of Cd8+ t cell receptor (Tcr) engineered therapies for the treatment of cancer. *Cells* 2021;10:2379:1-19.
- 3 van der Lee DI, Reijmers RM, Honders MW, et al. Mutated nucleophosmin 1 as immunotherapy target in acute myeloid leukemia. *J Clin Invest* 2019;129:97482:774-85.
- 4 van Amerongen RA, Hagedoorn RS, Remst DFG, et al. Wt1- specific TCRs directed against newly identified peptides install antitumor reactivity against acute myeloid leukemia and ovarian carcinoma. *J Immunother Cancer* 2022;10:e004409.
- 5 de Rooij MAJ, Remst DFG, van der Sten DM, et al. A library of cancer testis specific T cell receptors for T cell receptor gene therapy. *Mol Ther Oncolytics* 2023;28:1-14.
- 6 Chan JD, Lai J, Slaney CY, et al. Cellular networks controlling T cell persistence in adoptive cell therapy. *Nat Rev Immunol* 2021;21:769-84.
- 7 Singh H, Figliola MJ, Dawson MJ, et al. Reprogramming Cd19-specific T cells with IL-21 signaling can improve adoptive immunotherapy of B-lineage malignancies. *Cancer Res* 2011;71:3516-27.
- 8 Hinrichs CS, Borman ZA, Cassard L, et al. Adoptively transferred effector cells derived from naive rather than central memory Cd8+ T cells mediate superior antitumor immunity. *Proc Natl Acad Sci U S A* 2009;106:17469-74.
- 9 John LB, Devaud C, Duong CPM, et al. Anti-PD-1 antibody therapy potently enhances the eradication of established tumors by gene-modified T cells. *Clin Cancer Res* 2013;19:5636-46.
- 10 Stomper J, Rotondo JC, Greve G, et al. Hypomethylating agents (HMA) for the treatment of acute myeloid leukemia and myelodysplastic syndromes: mechanisms of resistance and novel HMA-based therapies. *Leukemia* 2021;35:1873-89.
- 11 Loo Yau H, Bell E, Ettayebi I, et al. DNA hypomethylating agents increase activation and cytolytic activity of Cd8+ T cells. *Mol Cell* 2021;81:1469-83.
- 12 Krishnadas DK, Bao L, Bai F, et al. Decitabine facilitates immune recognition of sarcoma cells by upregulating CT antigens, MHC molecules, and ICAM-1. *Tumour Biol* 2014;35:5753-62.
- 13 Dubovsky JA, McNeel DG, Powers JJ, et al. Treatment of chronic lymphocytic leukemia with a hypomethylating agent induces expression of Nxf2, an immunogenic cancer testis antigen. *Clin Cancer Res* 2009;15:3406-15.
- 14 Wang L, Amoozgar Z, Huang J, et al. Decitabine enhances lymphocyte migration and function and synergizes with CTLA-4 blockade in a murine ovarian cancer model. *Cancer Immunol Res* 2015;3:1030-41.
- 15 Langston SP, Grossman S, England D, et al. Discovery of TAK-981, a first-in-class inhibitor of SUMO-activating enzyme for the treatment of cancer. *J Med Chem* 2021;64:2501-20.
- 16 Biederstädt A, Hassan Z, Schneeweis C, et al. SUMO pathway inhibition targets an aggressive pancreatic cancer subtype. *Gut* 2020;69:1472-82.
- 17 Kumar S, Schoonderwoerd MJA, Kroonen JS, et al. Targeting Pancreatic cancer by TAK-981: a Sumoylation inhibitor that activates the immune system and blocks cancer cell cycle progression in a preclinical model. *Gut* 2022;71:2266-83.
- 18 Lightcap ES, Yu P, Grossman S, et al. A small-molecule sumoylation inhibitor activates antitumor immune responses and potentiates immune therapies in preclinical models. *Sci Transl Med* 2021;13:eaba7791.
- 19 Demel UM, Wirth M, Yousefian S, et al. Small molecule SUMO inhibition for biomarker-informed B-cell lymphoma therapy. *Haematol* 2022;108:555-67.
- 20 Demel UM, Böger M, Yousefian S, et al. Activated sumoylation restricts MHC class I antigen presentation to confer immune evasion in cancer. *J Clin Invest* 2022;132:e152383.
- 21 Borgermann N, Ackermann L, Schwertman P, et al. Sumoylation promotes protective responses to DNA-protein crosslinks. *EMBO J* 2019;38:e101496.
- 22 Kroonen JS, de Graaf IJ, Kumar S, et al. Inhibition of sumoylation enhances DNA hypomethylating drug efficacy to reduce outgrowth of hematopoietic malignancies. *Leukemia* 2023;37:864-76.
- 23 Döhner H, Weisdorf DJ, Bloomfield CD. Acute myeloid leukemia. *N Engl J Med* 2015;373:1136-52.
- 24 Bird SA, Boyd K. Multiple myeloma: an overview of management. *Palliat Care Soc Pract* 2019;13:1178224219868235.
- 25 Heemskerk MHM, Hoogeboom M, de Paus RA, et al. Redirection of antileukemic reactivity of peripheral T lymphocytes using gene transfer of minor histocompatibility antigen HA-2-specific T-cell receptor complexes expressing a conserved alpha joining region. *Blood* 2003;102:3530-40.
- 26 Jahn L, Hombrink P, Hagedoorn RS, et al. TCR-based therapy for multiple myeloma and other B-cell malignancies targeting intracellular transcription factor Bob1. *Blood* 2017;129:1284-95.
- 27 The high throughput RNA sequencing dataset is available in the gene expression omnibus (GEO) from NCBI with accession number GSE267689.
- 28 Ivashkin LB. IFN γ : signalling, epigenetics and roles in immunity, metabolism, disease and cancer Immunotherapy. *Nat Rev Immunol* 2018;18:545-58.
- 29 Decque A, Joffre O, Magalhaes JG, et al. Sumoylation coordinates the repression of inflammatory and anti-viral gene-expression programs during innate sensing. *Nat Immunol* 2016;17:140-9.
- 30 Adoriso S, Fierabracci A, Muscarì I, et al. SUMO proteins: guardians of immune system. *J Autoimmun* 2017;84:21-8.
- 31 Ma R, Rei M, Woodhouse I, et al. Decitabine increases neoantigen and cancer testis antigen expression to enhance T-cell-mediated toxicity against glioblastoma. *Neuro Oncol* 2022;24:2093-106.
- 32 Yang H, Bueso-Ramos C, DiNardo C, et al. Expression of PD-L1, PD-L2, PD-1 and Ctl4 in myelodysplastic syndromes is enhanced by treatment with hypomethylating agents. *Leukemia* 2014;28:1280-8.
- 33 Huang KC-Y, Chiang S-F, Chen WT-L, et al. Decitabine augments chemotherapy-induced PD-L1 upregulation for PD-L1 blockade in colorectal cancer. *Cancers (Basel)* 2020;12:462.
- 34 Liu Y, Zhou N, Zhou L, et al. IL-2 regulates tumor-reactive Cd8+ T cell exhaustion by activating the aryl hydrocarbon receptor. *Nat Immunol* 2021;22:358-69.
- 35 Wherry EJ, Kurachi M. Molecular and cellular insights into T cell exhaustion. *Nat Rev Immunol* 2015;15:486-99.
- 36 Gaissmaier L, Elshiaty M, Christopoulos P. Breaking bottlenecks for the TCR therapy of cancer. *Cells* 2020;9:2095.

supplement

**Targeting epigenetic regulation and post-translational
modification with 5-Aza-2' deoxycytidine and SUMO E1
inhibition Augments T Cell Receptor Therapy**

Jessie S. Kroonen¹, Anne K. Wouters², Ilona J. de Graaf¹, Dennis F.G. Remst², Sumit Kumar¹,
Tassilo L. A. Wachsmann², Amina Teunisse¹, Jessica Roelands³, Noel F. C. C. de Miranda³,
Marieke Griffioen², Mirjam H. M. Heemskerk^{2#}, Alfred C. O. Vertegaal^{1#}

¹Department of Chemical and Cell Biology, Leiden University Medical Centre, Leiden, The
Netherlands

²Department of Hematology, Leiden University Medical Centre, Leiden, The Netherlands

³Department of Pathology, Leiden University Medical Centre, Leiden, The Netherlands

shared senior and corresponding authors M.H.M.Heemskerk@lumc.nl; vertegaal@lumc.nl

Reagents table

Reagent or Resource	Source	Catalogue number	Dilution
Antibodies western blot			
SUMO1 mouse monoclonal	Cell Signaling Technology	21C7, Cat# 33-2400 RRID:AB_2198257	1/1000
SUMO2/3 mouse monoclonal	Universit of Iowa	8A2: RRID: AB_2198421	1/500
p-STAT Tyr701 rabbit monoclonal	Cell Signaling Technology	Cat# 9167; RRID: AB_561284	1/1000
β-actin mouse monoclonal	Sigma-Aldrich	Cat#: A5441 RRID: AB_476744	1/1000
Ubiquitin sc8017	Santa Cruz	Cat# sc-8017; RRID:AB_628423	1/5000
Antibodies Flowcytometry			
CD8 - FITC	BD biosciences	Cat# 555366 clone RPA-T8	1/40
Sytox - PacificBlue	BD biosciences	Lot 2369078	1/1000
Viability - ZombieRed	Biolegend	Cat# 423110 Lot B356980	1/1000
LAG-3 (CD223) - PerCP efluor 710	Invitrogen	Cat# 46-2239-42 Lot 2404262 Clone 3DS223H	1/80
hCD45 - V500	BD biosciences	Cat# 560777 Lot1088708 CLONE HI30	1/80
CD38 – BV605	BD biosciences	Cat# 740401 Lot 2101710 Clone HIT2	1/120
PD-1 (297) – BV786	BD biosciences	Cat# 563789 Lot 2060437 Clone EH12.1	1/100
HLA DR – Alexa700	BD biosciences	Cat# 560743 Lot 1313902 Clone F46-6	1/150
Ki67 – PECy7	BD biosciences	Cat# 561283 Lot 1211447 Clone B56	1/100
HLA A*02 – FITC	BD biosciences	Cat# 551285 Lot 1165046 Clone BB7.2	1/100
CD137 – APC	BD biosciences	Cat# 550890 Lot 1243782 Clone 4B4-1	1/75
mCD45 – PECy5	BD biosciences	Cat# 553082 Lot 1298554 Clone 30-F11	1/150
CD45 RA – PE Texas red	Invitrogen	Cat# MHCD45RA17 Lot 2206152 Clone MEM-56	1/200
CD8 – APC/H7	BD biosciences	Cat# 560179 lot2025113 clone SK1	1/250
CD25 – BV711	BD biosciences	Cat# 740776 Lot 2101714 Clone M-A251	1/100
PD-1L (CD274) – BV421	BD biosciences	Cat# 563738 Lot 9136926 Clone MIH1	1/40
ICOS – BV650	BD biosciences	Cat# 563832 Lot 2068020 Clone DX29	11/40
IRF-1 PE	BD biosciences	Cat# 566322 Lot 1270370 Clone 20/IRF-1	1/400

Brilliant stain buffer plus	BD biosciences	Cat# 566385 Lot 1307618	1/20
Compounds			
TAK981	Chemietek	CT-TAK981	
5-Aza-2'-deoxycytidine	Merck	A3656	
(2-Hydroxypropyl)-β-cyclodextrin (HPBCD)	Merck	H107	
qPCR primers	Primer ordered	Sequence source if external	
IFNγ FW GAGTGTGGAGACCATCAAGGAAG IFNγ Rev TGCTTTGCGTTGGACATTCAAGTC	Sigma	HP200586 OriGene	
IFN-β Fw GACATCCCTGAGGAGATTAAGCA IFN-β Rev CAACAATAGTCTCATTCCAGCCA	Sigma	Dr. Jochemsen (CCB, LUMC, NL)	
IFN-α Fw AGAAGGCTCCAGCCATCTCTGT IFN-α Rev TGCTGGTAGAGTTCGGTGCAGA	Sigma	HP214678 Origene	
TNF-α Fw CTCTTCTGCCTGCTGCACTTTG TNF-α Rev ATGGGCTACAGGCTTGCTACTC	Sigma	HP200561 Origene	
IFITM3 FW ATGTCGTCTGGTCCCTGTTC IFITM3 Rev GTCATGAGGATGCCAGAAT	Sigma	¹	
IRF7 FW TGGTCCTGGTGAAGCTGGAA IRF7 Rev GATGTCGTCATAGAGGCTTTGG	Sigma	¹	
STAT1-FW CAGCTTGACTCAAAATTCCTGGA STAT1-Rev TGAAGATTACGCTTGCTTTTCCT	Sigma	¹	
IFIT-1 FW GCCTTGCTGAAGTGTGGAGGAA IFIT-1 Rev ATCCAGGCGATAGGCAGAGATC	Sigma	HP226398 Origene	
ISG15 FW CAGCGAACTCATCTTTGCCAGTA ISG15 Rev CCAGCATCTTCACCGTCAGG	Sigma	Dr. Jochemsen (CCB, LUMC, NL)	
ISG56 Fw GGGCAGACTGGCAGAAGC ISG56 Rev TATAGCGGAAGGATTGAAAGC	Sigma	Dr. Jochemsen (CCB, LUMC, NL)	
IFNAR1 FW TTGGTGCAAGAGGAAGAAGAA IFNAR1 Rev GTGACAGAGACCACCCATAAC	Sigma	¹	
IL2 FW ACCAGGATGCTCACATTTAAGTTT IL2 Rev TCCCTGGGTCTTAAGTGAAAGTTT	Sigma	¹	
Perforin1 FW ACTCACAGGCAGCCAACTTTGC Perforin1 Rev CTCTTGAAGTCAGGTGCAGCG	Sigma	HP227388 Origene	
GranzymeB FW CGACAGTACCATTGAGTTGTGCG GranzymeB Rev TTCGTCCATAGGAGACAATGCC	Sigma	HP207492 Origene	
T-bet FW ATTGCCGTGACTGCCTACCAGA T-bet Rev	Sigma	HP210499 Origene	

GGAATTGACAGTTGGGTCCAGG			
IL-4 FW CCGTAACAGACATCTTTGCTGCC IL-4 Rev GAGTGTCTTCTCATGGTGGCT	Sigma	HP200556 Origene	
IL-5 FW GGAATAGGCACACTGGAGAGTC IL-5 Rev CTCTCCGTCCTTCTTCTCCACAC	Sigma	HP200819 Origene	
IL-10 FW TCTCCGAGATGCCTTCAGCAGA IL-10 Rev TCAGACAAGGCTTGGCAACCCA	Sigma	HP200540 Origene	
SRPR FW CATTGCTTTTGACGTAACCAA SRPR Rev ATTGTCTGCATGCGGCC	Sigma	Dr. Jochemsen (CCB, LUMC, NL)	
SDHA FW GCATTTGGCCTTTCTGAGGC SDHA Rev CTCCATGTTCCCCAGAGCAG	Sigma	²	
18s-RNA FW GGAGTATGGTTGCAAAGCTGA 18s-RNA Rev ATCTGTCAATCCTGTCCGTGT	Sigma	Dr. Jochemsen (CCB, LUMC, NL)	

Materials and Methods

Compounds

5-Aza-2'-deoxycytidine (5-Aza-2', Merck) was dissolved in DMSO for *in vitro* usage and in 20% (2-Hydroxypropyl)-β-cyclodextrin (HPBCD, Merck) for *in vivo* purposes. TAK981 (Chemietek) was dissolved in DMSO for *in vitro* usage and in 20% HPBCD for *in vivo* purposes. 5-Aza-2'-deoxycytidine (5-Aza-2', Merck) was dissolved in DMSO for *in vitro* usage and in 20% HPBCD for *in vivo* purposes.

Cell culture

OCI-AML3 cells (HLA-A*02:01+ mutant NPM1+ HA2+) were obtained from DSMZ (Braunschweig, Germany) and U266 cell line (HLA-A*02:01+, HLA-B*07:02+, BOB1+, MAGE-A1+) was obtained from Prof. Dr T. Mutis (Department of Hematology, VUMC, NL). Cell lines were cultured in IMDM (Lonza), supplemented with 1.5% glutamine (Lonza), 10% fetal bovine serum (Gibco, Life Technologies) and 1% Penicillin-Streptomycin (Lonza). Cells were cultured at 37 °C and 5% CO₂ in a humidified incubator.

T cells were cultured in IMDM (Lonza) supplemented with 5% fetal bovine serum (FBS; Gibco, Life Technologies), 5% human serum, 1.5% glutamine (Lonza), 1% penicillin/streptomycin (Lonza), and

100 IU/ml IL-2 (Proleukin; Novartis Pharma), herein referred to as T cell medium (TCM). CD8⁺ T cells were isolated from healthy donor peripheral blood mononuclear cells (PBMCs) by MACS using anti-CD8 MicroBeads (Milenyi Biotec). CD8⁺ T cells were subsequently activated with irradiated autologous PBMCs (35 Gy) and 0.8 mg/mL phytohemagglutinin (PHA; Oxoid Microbiology Products, Thermo Fisher Scientific), and cultured in TCM. PBMCs were obtained from the Leiden University Medical Center Biobank for Hematological Diseases (approval number B16.039). Samples were collected after written informed consent.

TCR transfer to healthy donor T cells

On day 2 post activation, CD8⁺ T cells were retrovirally transduced with NPM1-TCR^{(CLA A2)3}, HA2-TCR^{(YIG A2)4}, BOB1/4G11-TCR^{(APA B7)5}, MAGE-A1-TCR^{(KVL A2)6} or CMV-TCR^{(NLV A2)3}, using 24-well non-tissue culture plate coated with retronectin (30 mg/mL) (Takara) overnight at 4°C. Wells were blocked with 2% human serum albumin (HSA) (Sanquin) for 30 min. Viral supernatant was thawed and added to the 24-wells plate and spun for 20 min, 2,000g at 4°C. Virus supernatant was removed and 0.3*10⁶ activated CD8⁺ T cells were transferred to each well. After overnight incubation, T cells were transferred to a tissue culture plate. On day 7 post activation TCR transduced T cells were indirectly MACS enriched for introduced TCR expression on anti-mouse TCR-C β APC antibody (mTCR APC; BD Pharmingen) followed by anti-APC MicroBeads (Milenyi Biotec). Purified T cells were used in experiments between day 10-14 after activation. TCR expression was assessed by HLA tetramer binding; cells were stained for anti-mTCR APC antibody and PE labeled pHLA-tetramers. Cells were measured on the LSR II (BD Bioscience), and data were analyzed with FlowJo Version 10 software.

Viability assay

OCI-AML3 and U266 cells were seeded in 96-well flat bottom plate format in a density of 1*10⁵ cells/mL. OCI-AML3 cells were treated for 4 days with increasing concentrations of TAK981 (0.0001 – 0.1 μ M) or 5-Aza-2' (0.025 – 20 μ M) as indicated in the figures; 0.01% DMSO was used as control. For

synergy analysis, a dose range of 5-Aza-2' (0.025 – 0.10 μ M) with or without 0.01 μ M of TAK981 was used. For synergy response of U266, cells were treated with a dose range of 5-Aza-2' (1.5 – 20 μ M) with or without 0.25 μ M of TAK981. Presto Blue viability reagent (A13261, Merck) was added 1:10 into cell culture medium for 1 hour at 37°C and 5% CO₂. Fluorescence was measured with a plate reader (Victor X3, Perkin Elmer) at 544/591nm. Three technical replicates were used within each of three biological replicates performed for the viability assays performed. The excess overbliss model⁷ was used to calculate the synergistic score, using the following formula with Fa as the fractional activity: Excess overbliss = $(Fa_1 + Fa_2 - [(Fa_1 \times Fa_2)]) \times 100$.

Western Blot

Total cell lysates of OCI-AML3 and U266 cells treated with TAK981 (0.05 to 1 μ M) or DMSO 0.01% were analyzed by western blotting for SUMO2/3, SUMO1 and conjugation. CD8+ T cells treated with 100 nM TAK981 and/or 250 nM 5-Aza-2' overnight were analyzed by western blotting for p-STAT Tyr701 and SUMO2/3 and β -actin for loading control. Total lysates were prepared on ice in RNP buffer (2% SDS, 1% NP40, 50mM Tris pH 7.5, 150 mM NaCl) followed by 10 min at 100°C. Proteins were size separated with precast 4-12% Bis-Tris gradient gels (Thermo Fisher Scientific). Size-separated proteins were transferred to nitrocellulose membranes (0.45 μ m, Amersham Protran Premium (Merck)). Membranes were incubated with primary antibodies against SUMO2/3 (1:500, mouse monoclonal 8A2, University of Iowa), SUMO1 (1:1000, 4930P, Cell Signaling Technology), ubiquitin (1:5000, sc8017, Santa Cruz), and β -actin in 5% milk powder in PBS - 0.05% Tween20. Membranes were incubated with p-STAT1 Tyr701 (1:1000, 58D6, Cell Signaling Technology) antibody in TBS – 0.05% Tween20 – 3% bovine serum albumin. Goat anti- mouse IgG- HRP (1:2500) and Donkey anti- rabbit IgG- HRP (1:10 000) were used as secondary antibodies in 5% milk in TBS – 0.05% Tween20 – 3% bovine serum albumin. ECL signal was detected using Pierce ECL2 (Life Technologies) and imaged using the iBright CL1500 (Invitrogen iBright Imaging Systems).

qPCR

CD8+ T cells from three healthy donors were cultured in TCM and treated with 10 and 100 nM TAK981 and/or 25 and 250 nM 5-Aza-2' or control DMSO 0.01% overnight, 10 days post stimulation. Total RNA of CD8+ T cells was isolated with use of SV total RNA isolation system (Promega). 0.5 – 1 µg of RNA was used for cDNA synthesis using random primers (Invitrogen) and reverse transcriptase ImProm-II (Promega) following manufacturer's protocol. Real-time quantitative PCR was performed with SYBR Green PCR Mastermix (Applied Biosystems) on a CFX384 real-time PCR detection system (Bio-Rad) according to the following protocol. 95 °C for 7 minutes, followed by 39 cycles of; 95 °C 15 seconds, 60 °C 15 seconds, 60 °C 35 seconds + measurement, the protocol was finalized with 95 °C 10 seconds, 65 °C 5 seconds + measurement and 95 °C 50 seconds. CT values of genes were normalized against the geometric mean of housekeeping genes (SRPR, 18S-RNA and SDHA). Primer sequences are listed in the reagent table.

Co-culture IFN γ ELISA

5000 CD8+ T cells (NPM1-TCR, CMV-TCR) were co-cultured with OCI-AML3 as target cells in an E:T ratio of 1:6. CD8+ T cells or OCI-AML3 target cells were pre-treated with 10 nM TAK981 and/or 250 nM 5-Aza-2' or 0.01% DMSO control, on day 10 and 14 post stimulation of CD8+ T cells. Subsequently OCI-AML3 and CD8+ T cells were washed and co-cultured overnight in 60 µL of TCM. Supernatant was harvested, diluted 5x and 125x and, IFN γ was measured by ELISA according to manufacturer's instructions adapted for 384 well plates (Diacclone).

CD8+ survival assay

Activated CD8+ T cells (NPM1-TCR, CMV-TCR, HA2.5-TCR) were co-cultured with irradiated (50Gy) target cells (OCI-AML3, OCI-AML2) for 5 and 7 days in 96-well round bottom plates in an E:T ratio of 1:5 (5,000 CD8+ T cells). During co-culture, cells were treated on day 1 and 4 with 10 nM TAK981 and/or 250 nM 5-Aza-2' or DMSO 0.01% as control. CD8+ T cell counts were measured with help of

flow cytometry (LSR-II). Cells were spun down in plates and CD8+-FITC conjugated ab (BD Pharmingen) was added for 30 min. Subsequently, cells were washed with PBS and resuspended in SytoxBlue (Thermofisher) dead marker (1:1000). Target cells have an internal label of tdTomato, which was used for identification. Each sample was run for a standardized time of 23 seconds. CD8+ T cells were gated out as presented in supplementary figure 3 and total counts were used for analysis.

***in vivo* tumor therapy**

In vivo studies performed were approved by the national Ethical Committee for Animal Research (AVD116002017891). OCI-AML3-Luc and U266-Luc cells were transduced with Luciferase-tdTomato. Cell lines were bulk enriched for tdTomato expression using an Aria III cell sorter (BD Biosciences) to reach >98% purity. Male and female NOD *scid* gamma (NSG) mice (NOD.Cg-Prkdc(scid) Il2rg(tm1Wjl)/SzJ) originated from the Jackson Laboratory and were bred in house. Male NSG mice were inoculated with 1×10^6 OCI-AML3-Luc cells intravenously (i.v.). Male and female NSG mice were inoculated with 2×10^6 U266-Luc (multiple myeloma) cells i.v.

Tumor growth was measured bi-weekly with use of the In Vivo Imaging System (IVIS-spectrum, Perkin Elmer). Mice were subcutaneously injected with 150 μ L of 7.5 mM D-luciferin potassium salt (Synchem) and bioluminescence (photons/sec/cm²/r) of U266-LUC and OCI-AML3 cells was measured.

Treatment with TAK981 (25mg/kg) and/or 5-Aza-2' (2.5mg/kg) or HPBCD-buffer as control was started on day 10 or day 14 post inoculation of OCI-AML3 and U266 respectively. Maximum weight of mice used for drug doses calculation was set to 20gram. For the OCI-AML3 model, 3×10^6 NPM1-TCR, HA2-TCR or CMV-TCR T cells were injected i.v. on day 15. For the U266 model, 1×10^6 BOB1-TCR, MAGE-A1-TCR or CMV-TCR T cells were injected i.v. on day 19. Drug treatment was continued bi-weekly until day 50 post tumor inoculation.

In vivo NPM1-TCR CD8+ T cell-LUC tracking

Male NSG-mice (n=6/group) were inoculated with 1×10^6 OCI-AML3 cells via i.v. injection. Treatment with TAK981 (25mg/kg) and/or 5-Aza-2' (2.5mg/kg) or HPBCD-buffer control was started on day 14 post inoculation of OCI-AML3 cells and continued bi-weekly. Maximum weight of mice used for drug doses calculation was set to 20gram. NPM1-TCR and CMV-TCR CD8+ T cells were transduced with Luciferase-tdTomato. CD8+ T cells were bulk enriched for tdTomato expression using an Aria III cell sorter (BD Biosciences) to reach >98% purity. On day 18 post OCI-AML3 injection 3×10^6 NPM1-TCR luc or CMV-TCR Luc CD8+ T cells were injected i.v.. T cell BLI was monitored on day 3, 6 and 9 post injection, using IVIS imaging following s.c. injection of 150 μ L of 7.5 mM D-luciferin.

Isolation of bone marrow and ex-vivo CD8+ T cell and tumor analysis

Bone marrow was harvested from euthanized mice on day 2 (n=4/group), day 5 (n=3/group) and day 8 (n=3/group). Femurs were cleaned of surrounding tissue and cut open on the knee-side. The open femurs were placed into a 1.5ml Eppendorf tube containing 100ul of T cell medium and spun down at 2500g at room temperature. Bone marrow suspension was filtered through a cell strainer (70 μ M) (sysmex) into a sterile tube. Subsequently, bone marrow was spun down (500g) and resuspended in 500 μ L red blood cell lysis buffer (154 mM ammoniumchloride) for 10 minutes on ice. Lysed samples were spun and supernatant was removed. Samples were transferred to round bottom 96-well plates for staining. 20 μ L of Zombie-red staining (Thermofisher) (1:1000 in PBS) was added to each well for 25 min. Plates were washed with PBS and 100 μ L of paraformaldehyde (1%) was added and incubated for 8 min at room temperature for fixation. Plates were spun and PFA was removed from samples; subsequently 100 μ L saponin-buffer (500 mL PBS, 2 mL 200g/L albumin, 1% P/S, 0.1% saponin (Quillaja)) was added and plates were incubated for 30 min at 4°C. After removal of the saponin-buffer, 20 μ L of antibody mix (reagent table) including BV staining buffer Buffer (BD Pharmingen) plus (1/20) and 5% normal mouse serum (Thermofisher) was added and incubated for 30 min at room temperature. Finally, plates were washed with saponin-buffer and the samples were resuspended in

50 μ L saponin-buffer and acquired on a Cytex Aurora spectral flow cytometer 3L (Cytekbio). Bone marrow of mice with only tumor was used as unstained samples.

Isolation of bone marrow and ex-vivo single cell tumor analysis

Bone marrow was harvested as stated above. For each mouse bone marrow of both paws was combined. Negative MACS enrichment of human cells of the bone marrow was performed, using anti-mCD45 (APC) and APC-beads. Enriched human cells from each mouse were labeled with unique hashtags (totalSeq-A human hashtags). Subsequently, to further purify the sample, anti-hCD45 was used to positive select human cells through sorting. Following 1 run of 10x Genomics 3' v3.1 chemistry was performed.

Single cell RNA sequencing

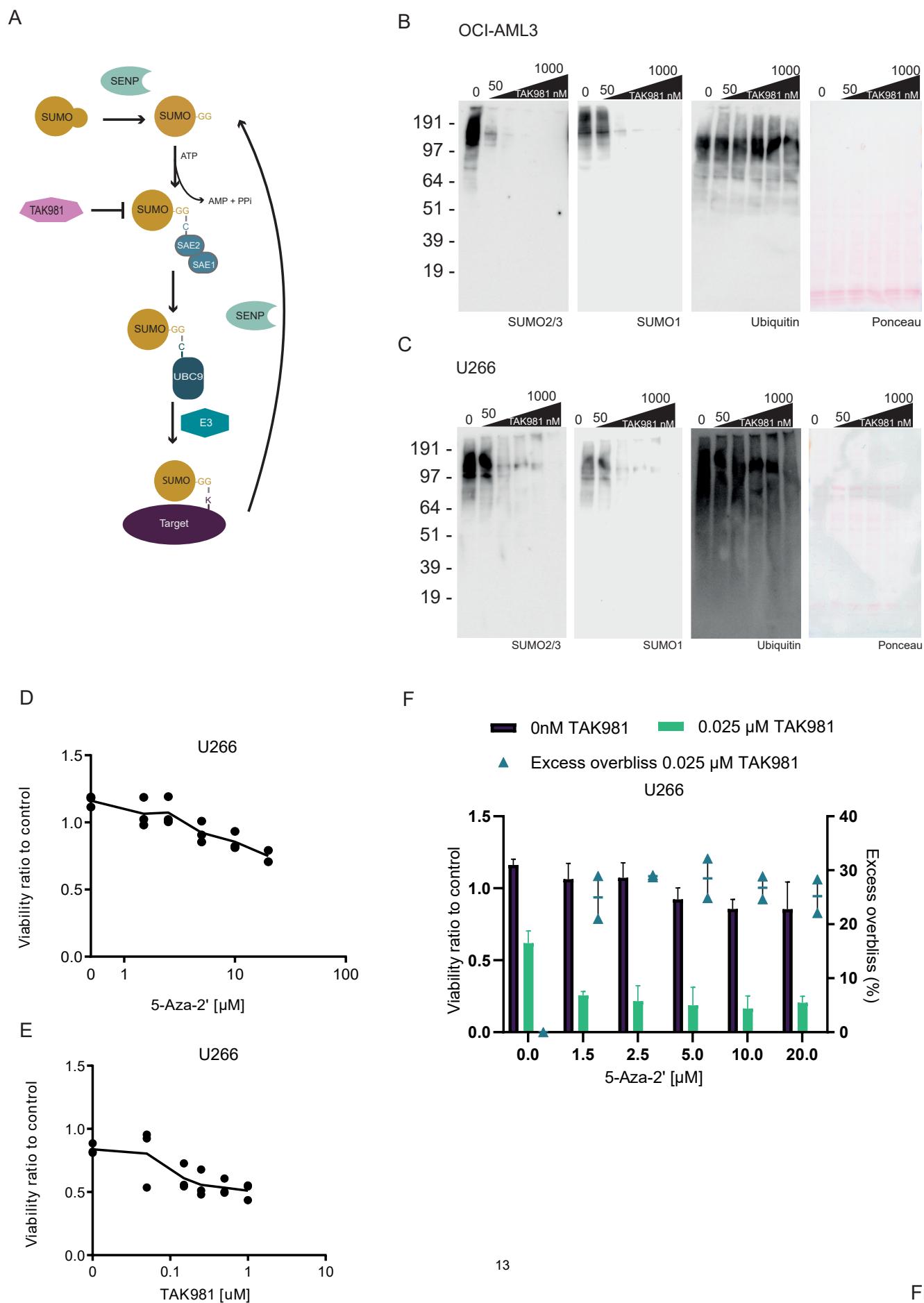
scRNA-seq was performed on sorted human cells. Single-cell gene expression libraries were prepared using the 10x Genomics Chromium X platform, specifically employing the Chromium Next GEM Single Cell 3' Library & Gel Bead Kit v3.1 and Chromium Next GEM Chip G Single Cell Kit (10x Genomics) according to manufacturer's instructions. Subsequently, the gene expression libraries were sequenced on a NovaSeq 6000 S4 flow cell with v1.5 chemistry (Illumina), and fastq files were generated using Cell Ranger mkfastq (10x Genomics). These fastq files were analyzed using the 10x Genomics Cell Ranger software version 7.0.0 and a custom reference with GRCh38-2020 containing the tdTomato gene. Raw data will be made available on GEO.

All downstream analysis was performed using Seurat (v.4.3.0). Samples were demultiplexed using hashtag oligos (HTO) by application of the 'MULTIseqDemux' function to identify singlets, doublets and negative cells⁸. Cells with a low number of expressed genes (<200) or high mitochondrial content (> 10%) were filtered out from the analysis. Data from a total of 2075 remaining cells was normalized using Seurat's 'LogNormalize' function with scaling factor set at 10,000. Variable features were identified using the 'FindVariableFeatures' function, resulting in the selection of 2,000 genes. To

visualize cells in a two-dimensional space, t-distributed stochastic neighbor embedding (t-SNE) was used. Differential gene expression was performed using the 'FindAllMarkers' function, with a min.pct of 0.25 and logfc. threshold at 0.25. We identified a cluster of 1795 tumor cells and a separate cluster of T cells based on expression of T cell genes and expression of tdTomato. T cell counts were insufficient for proper analysis and therefor excluded from the results. Data from all tumor cells were extracted and analyzed separately. Selected genes of interest associated with proliferation, MHC, cell surface molecules, and immune checkpoints were visualized per treatment condition using the 'DotPlot' function.

Supplementary References

1. Lightcap ES, Yu P, Grossman S, et al. A small-molecule SUMOylation inhibitor activates antitumor immune responses and potentiates immune therapies in preclinical models. *Sci Transl Med*. 2021;13(611):7791.
2. Geigges M, Gubser PM, Unterstab G, et al. Reference Genes for Expression Studies in Human CD8+ Naïve and Effector Memory T Cells under Resting and Activating Conditions. *Sci Reports* 2020 10:1. 2020;10(1):1–12.
3. van der Lee DI, Reijmers RM, Honders MW, et al. Mutated nucleophosmin 1 as immunotherapy target in acute myeloid leukemia. *J Clin Invest*. 2019;129(2):774–785.
4. Heemskerk MHM, Hoogeboom M, de Paus RA, et al. Redirection of antileukemic reactivity of peripheral T lymphocytes using gene transfer of minor histocompatibility antigen HA-2-specific T-cell receptor complexes expressing a conserved alpha joining region. *Blood*. 2003;102(10):3530–3540.
5. Jahn L, Hombrink P, Hagedoorn RS, et al. TCR-based therapy for multiple myeloma and other B-cell malignancies targeting intracellular transcription factor BOB1. *Blood*. 2017;129(10):1284–1295.
6. De Rooij MAJ, Remst DFG, Van Der Steen DM, et al. A library of cancer testis specific T cell receptors for T cell receptor gene therapy. *Mol Ther Oncolytics*. 2023;28:1–14.
7. Bliss CI. The calculation of microbial assays. *Bacteriol Rev*. 1956;20(4):243–258.
8. McGinnis C, Patterson DM, Winkler J, et al. MULTI-seq: sample multiplexing for single-cell RNA sequencing using lipid-tagged indices. *Nat Methods*. 2019;16(7):619–626.



Supplementary Figure 1 TAK981 and 5-Aza-2' synergistically reduce U266 viability. **A** The SUMOylation cycle. SUMO precursor protein is cleaved by SUMO specific proteases (SENPs) to produce mature SUMO. Target proteins are SUMOylated via an enzymatic cascade that consists of the E1 activating enzyme, the E2 conjugating enzyme and an E3 ligase. SUMO can be removed from a target protein by SENPs. Small molecule SUMOylation inhibitor TAK981 inhibits the E1 enzyme. **B** OCI-AML3 cells treated with TAK981 (50 – 1000 nM) or DMSO 0.01% control for 4 hours. Cells were lysed and analysed by immunoblotting for SUMO2/3, SUMO1 and ubiquitin. PonceauS staining was used as loading control. **C** U266 cells treated with 50 – 1000 nM of TAK981 or DMSO 0.01% control for 4 hours, were analysed for SUMO2/3, SUMO1 and ubiquitin protein expression via Western Blotting. PonceauS staining was used as loading control. **D** U266 cell viability is shown after 4 days of 5-Aza-2' treatment (0.025 – 20 μ M) or control DMSO 0.01% treatment (n=3). **E** U266 cell viability after 4 days of TAK981 treatment (0.05 – 1 μ M) or control DMSO 0.01% treatment. (n=3). **F** U266 cell viability after 4 days of combination treatment with dose response range of 5-Aza-2' with 25 nM of TAK981. Excess overbliss synergy calculations of single 5-Aza-2' doses versus 5-Aza-2' doses with 25 nM TAK981 are shown in the right y-axis per dose.

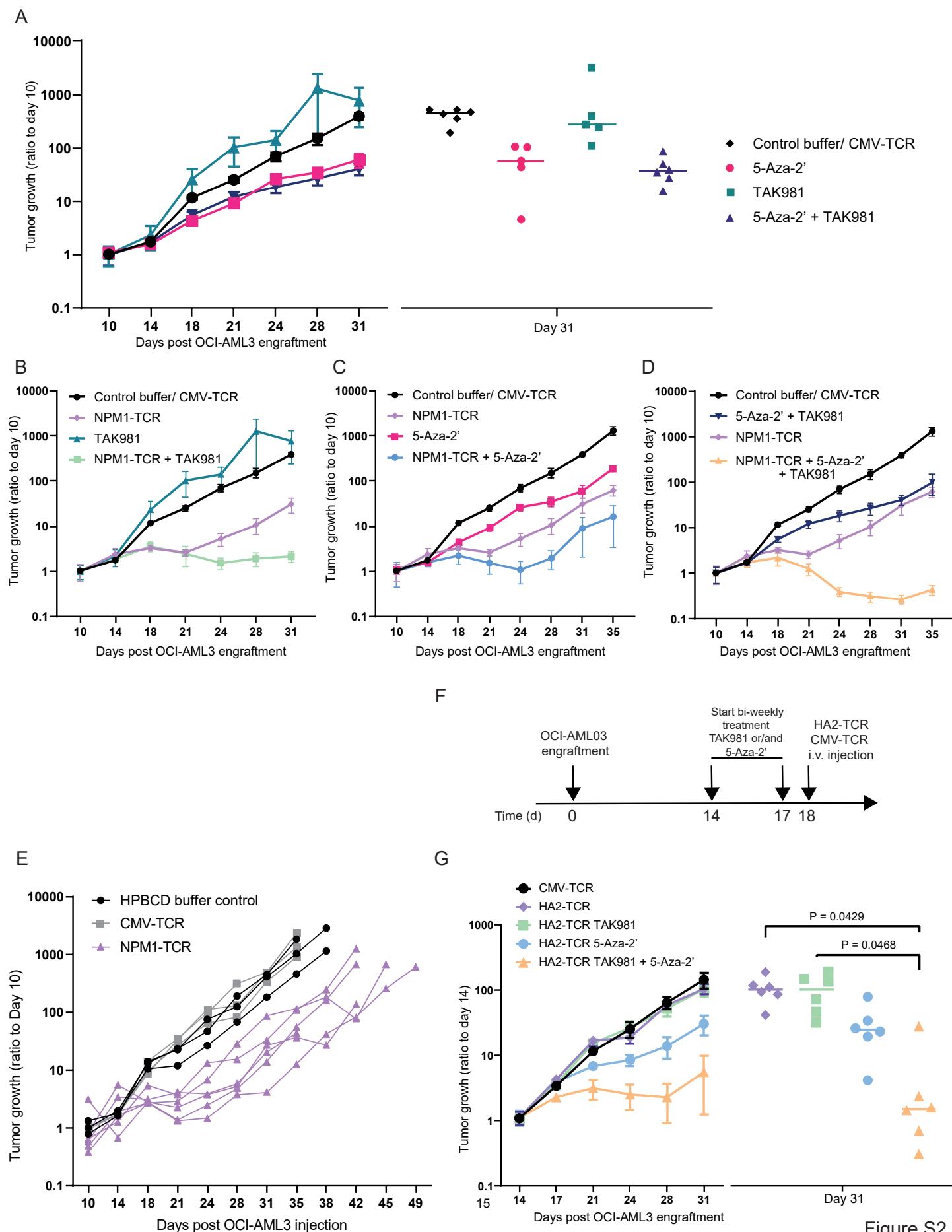
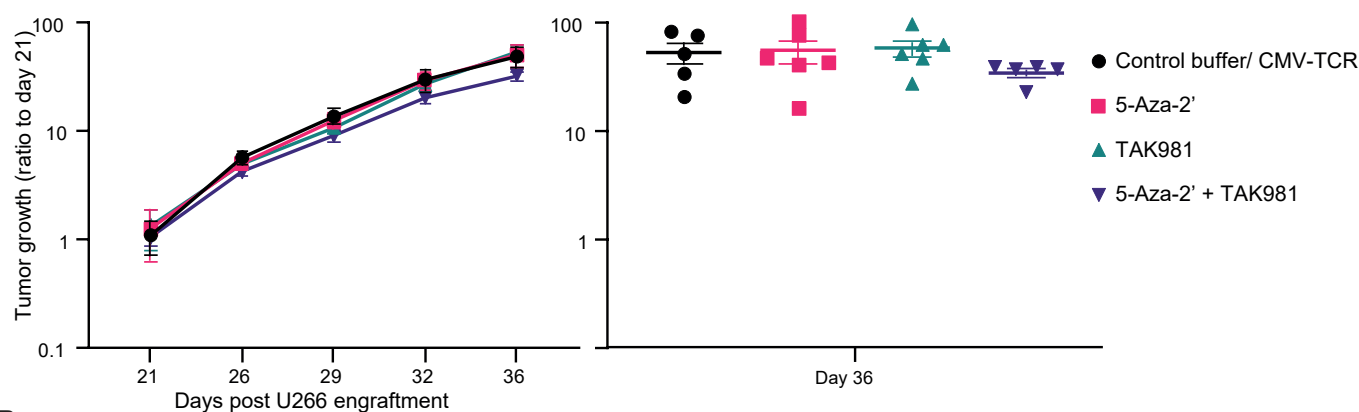
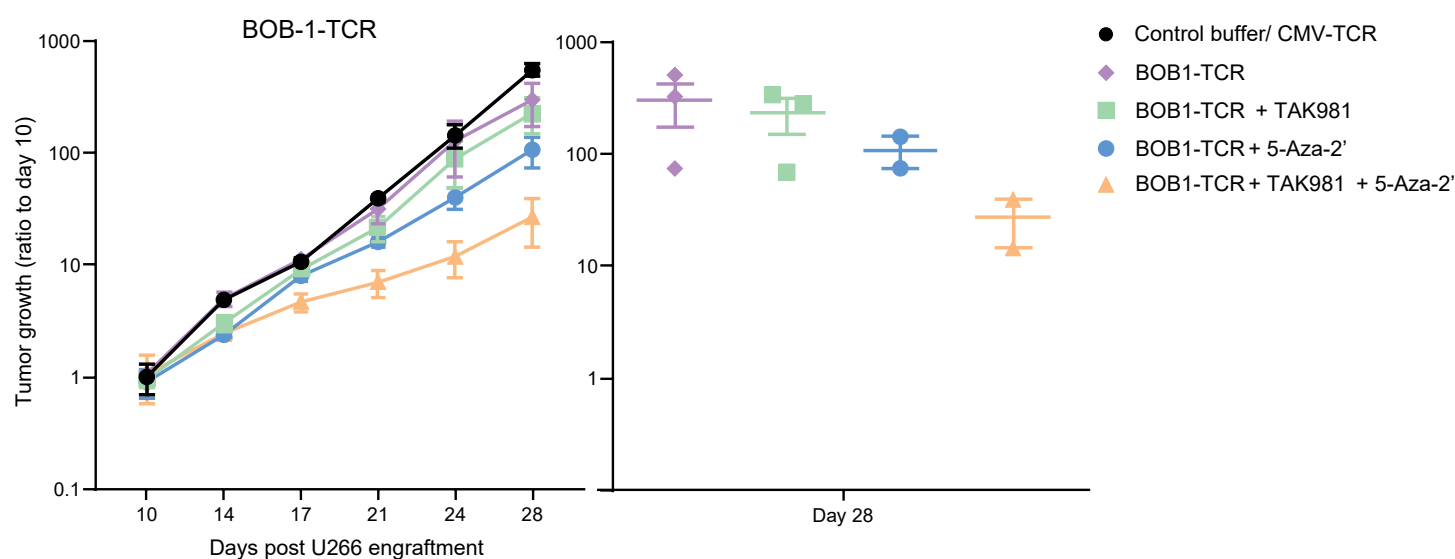
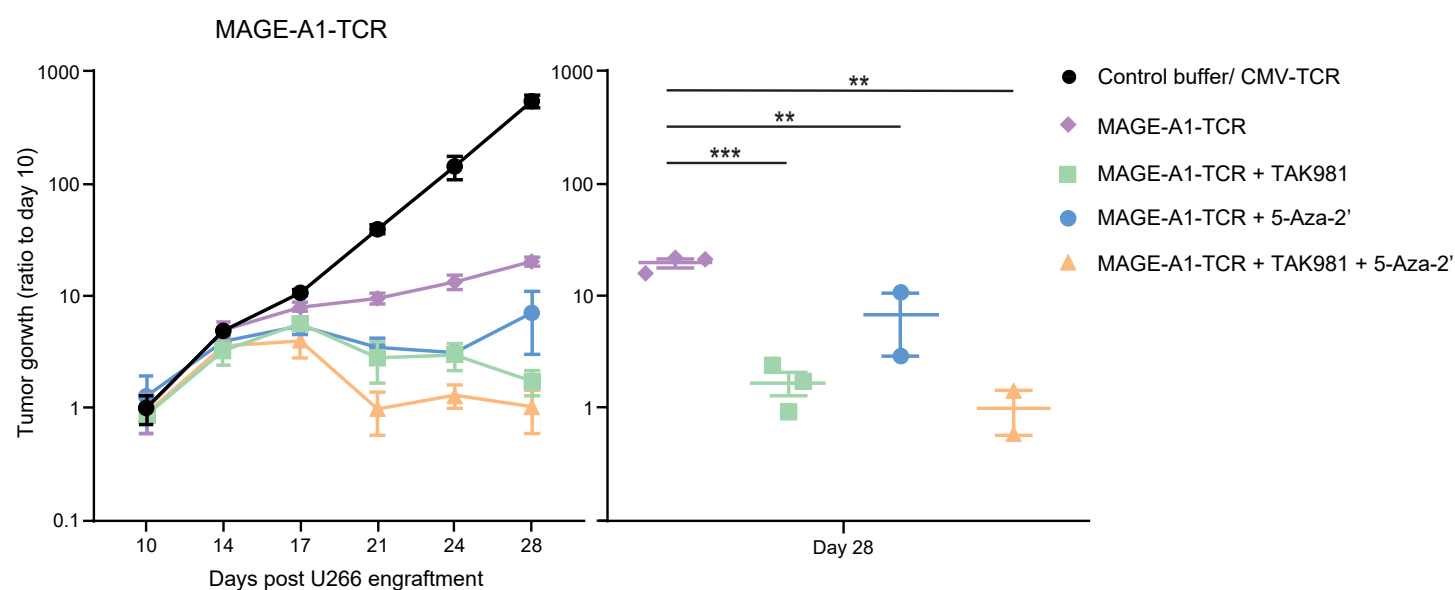


Figure S2

Supplementary Figure 2 NPM1-TCR CD8⁺ T cells and HA2-TCR CD8⁺ T cells anti-tumor efficacy is enhanced by 5-Aza-2' and TAK981 *in vivo*. **A** OCI-AML3 tumor outgrowth average per group (n=6); ratio to bioluminescent (BLI photons/sec/cm2/r) signal per mouse at day 10 is shown. Graphs represent time point when all mice were present in the experiment. Only compound groups from Figure 3B are shown. One-Way ANOVA analysis was performed for tumor signals at day 31, in GraphPad Prism 9.3.1. **B** TAK981 enhances tumor cell killing by NPM1-TCR. Data from Figure 3B. OCI-AML3 tumor outgrowth average per group (n=6) ratio to bioluminescent (BLI photons/sec/cm2/r) signal per mouse at day 10. Graphs represent time point when all mice were present in the experiment. **C** 5-Aza-2' enhances tumor cell killing by NPM1-TCR. Data from Figure 3B. OCI-AML3 tumor outgrowth average per group (n=6); ratio to bioluminescent (BLI photons/sec/cm2/r) signal per mouse at day 10. Graphs represent time point when all mice were present in the experiment. **D** TAK981 and 5-Aza-2' enhance tumor cell killing by NPM1-TCR. Data from Figure 3B. OCI-AML3 tumor outgrowth average per group (n=6) ratio to bioluminescent (BLI photons/sec/cm2/r) signal per mouse at day 10. Graphs represent time point when all mice were present in the experiment. **E** Control groups of Figure 2B & C, Supplementary Figure 2 A-D plotted separately to indicate the non-responsiveness of the control buffer and CMV-TCR to OCI-AML3 tumor compared to NPM1-CMV-TCR. **F** Timeline of *in vivo* experiment shown in Figure 3G. Luciferase expressing OCI-AML3 cells (1×10^6) were injected intra-venously (i.v.) into the tail vein of NSG-mice and engrafted for 14 days. Drug dosing was used as described in Figure 3A. HA2-TCR CD8⁺ T cells (3×10^6) were injected on day 18. **G** OCI-AML3 tumor outgrowth average per group (n=6); ratio to bioluminescent (BLI photons/sec/cm2/r) signal per mouse at day 10. Graphs represent time point when all mice were present in the experiment. One-Way ANOVA analysis was performed for tumor signals at day 31, in GraphPad Prism 9.3.1.

A**B****C**

Supplementary Figure 3 MAGE-A1 and BOB1-TCR CD8⁺ T cell anti-tumor efficacy in a multiple myeloma model (U266) is enhanced by 5-Aza-2' and TAK981 *in vivo*. Luciferase expressing U266 cells (2×10^6) expressing BOB1 and MAGE-A1 and positive for HLA-B*07:02 and HLA-A*02:01 were injected intra-venously (i.v.) into the tail vein of NSG-mice and engrafted for 14 days. Tumor volume was measured by IVIS. At day 14 treatment was started. Two rounds of the drug treatment with TAK981 (25 mg/kg) and/or 5-Aza-2' (2.5 mg/kg) were carried out. Subsequently 4G11/BOB1-TCR or MAGEA1-TCR CD8⁺ T cells (1×10^6) were i.v. injected on day 19. **A** U266-Luc tumor outgrowth per group (n=6) NSG (male) mice. Data is presented as ratio to bioluminescent (BLI photons/sec/cm²/r) signal per mouse at day 21. Graphs represent time point when all mice were present in the experiment. Only groups treated with compound are shown. One-Way ANOVA analysis was performed for tumor signals at day 36, in GraphPad Prism 9.3.1. **B** U266-Luc tumor outgrowth average per group (n=3) NSG (female) mice data is presented as ratio to bioluminescent (BLI photons/sec/cm²/r) signal per mouse at day 10 upon BOB1-TCR with or without TAK981 and/or 5-Aza-2'. One-Way ANOVA analysis was performed for tumor signals at day 28, in GraphPad Prism 9.3.1. **C** U266-Luc tumor outgrowth average per group (n=3) NSG (female) mice data is presented as ratio to bioluminescent (BLI photons/sec/cm²/r) signal per mouse at day 10 upon MAGE1-A2-TCR with or without TAK981 and/or 5-Aza-2'. One-Way ANOVA analysis was performed for tumor signals at day 28, in GraphPad Prism 9.3.1.

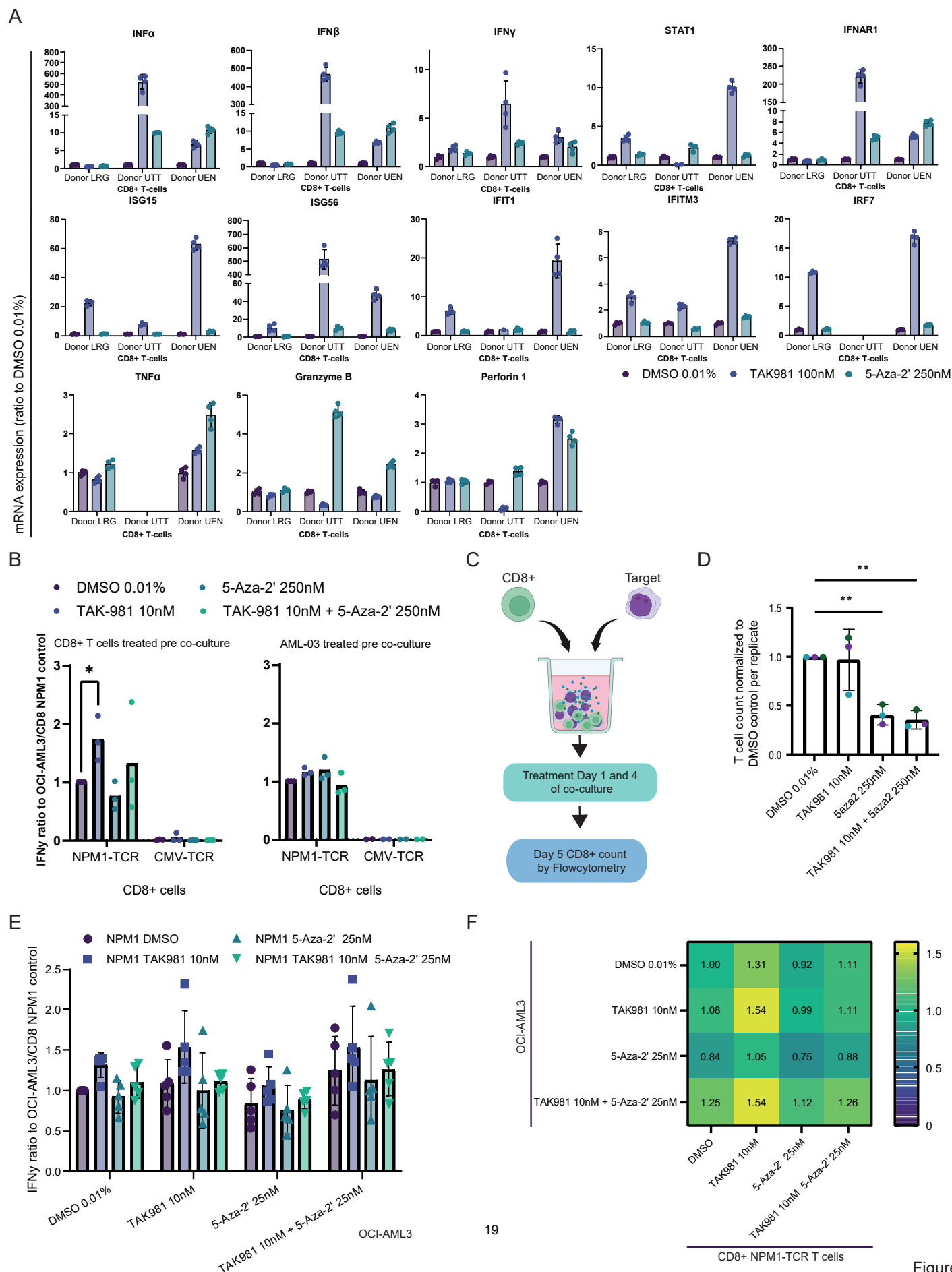


Figure S4

Supplementary Figure 4 Higher dosing of TAK981 and 5-Aza-2' increasingly activate interferon signalling, also causing more cytotoxicity. **A** mRNA expression levels of IFN α , IFN β , IFN γ , STAT1, IFNAR1, ISG15, ISG56, IFIT1, IFITM3, IRF7, TNF α , Granzyme B and Perforin 1 were measured using qPCR, for CD8+ T cells isolated from three different healthy donors. CD8+ T cells were treated 10 days post stimulation with 100 nM TAK981, 250 nM 5-Aza-2' or DMSO 0.01% as control overnight. 18sRNA, SDHA and SRPR were used as housekeeping genes. Expression was plotted as ratio to DMSO 0.01% control, individual per donor. **B** OCI-AML3 target cells or CD8+ T cells were pre-treated on day 1 and 4 with 10 nM TAK981 and/or 250 nM 5-Aza-2'. Subsequently, co-cultured with untreated OCI-AML3 or CD8+ NPM1-TCR T cells overnight. Supernatant was harvested and analysed by IFN γ ELISA. Three different donors were used for the generation of CD8+ NPM1-TCR T cells $P < 0.05 = *$, two-way ANOVA compared to DMSO 0.01%, followed by Fisher's LSD test, GraphPad Prism 9.3.1. **C** Experimental co-culture set up for CD8+ T cell survival upon TAK981 and/or 5-Aza-2' treatment, quantification by flow cytometry. **D** NPM1-TCR CD8+ T cell counts are shown upon 5 days of co-culture with irradiated OCI-AML3 cells (to prevent overgrowth). CD8+ T cells were treated with TAK981 at 10 nM and/or 5-Aza-2' at 250 nM or DMSO 0.01% control. Co-cultures were set up in T cell medium deficient of IL2. Data represent three different CD8+ T cell donor replicates. Each replicate is plotted individually as ratio to normalized DMSO control. **E** Extended data for Figure 3C and D. OCI-AML3 target cells or CD8+ T cells were pre-treated on day 1 and 4 with 10 nM TAK981 and/or 250 nM 5-Aza-2' or DMSO 0.01% as control. Subsequently, cells were co-cultured in all possible combinations of conditions. Supernatant was harvested and analysed by IFN γ ELISA. Five different donors were used for the generation of CD8+ NPM1-TCR T cells. **F** Heat map presentation of data from E.

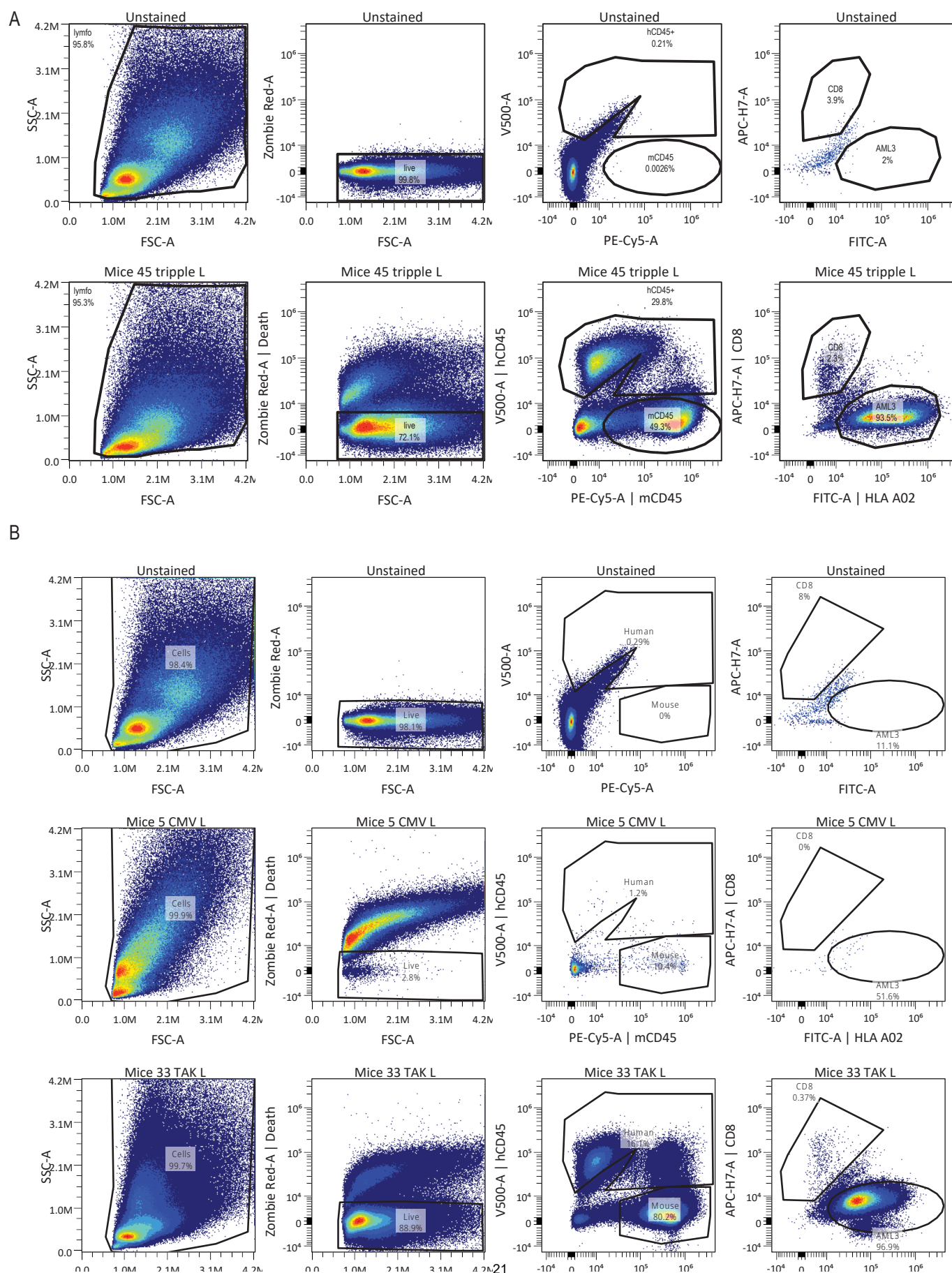
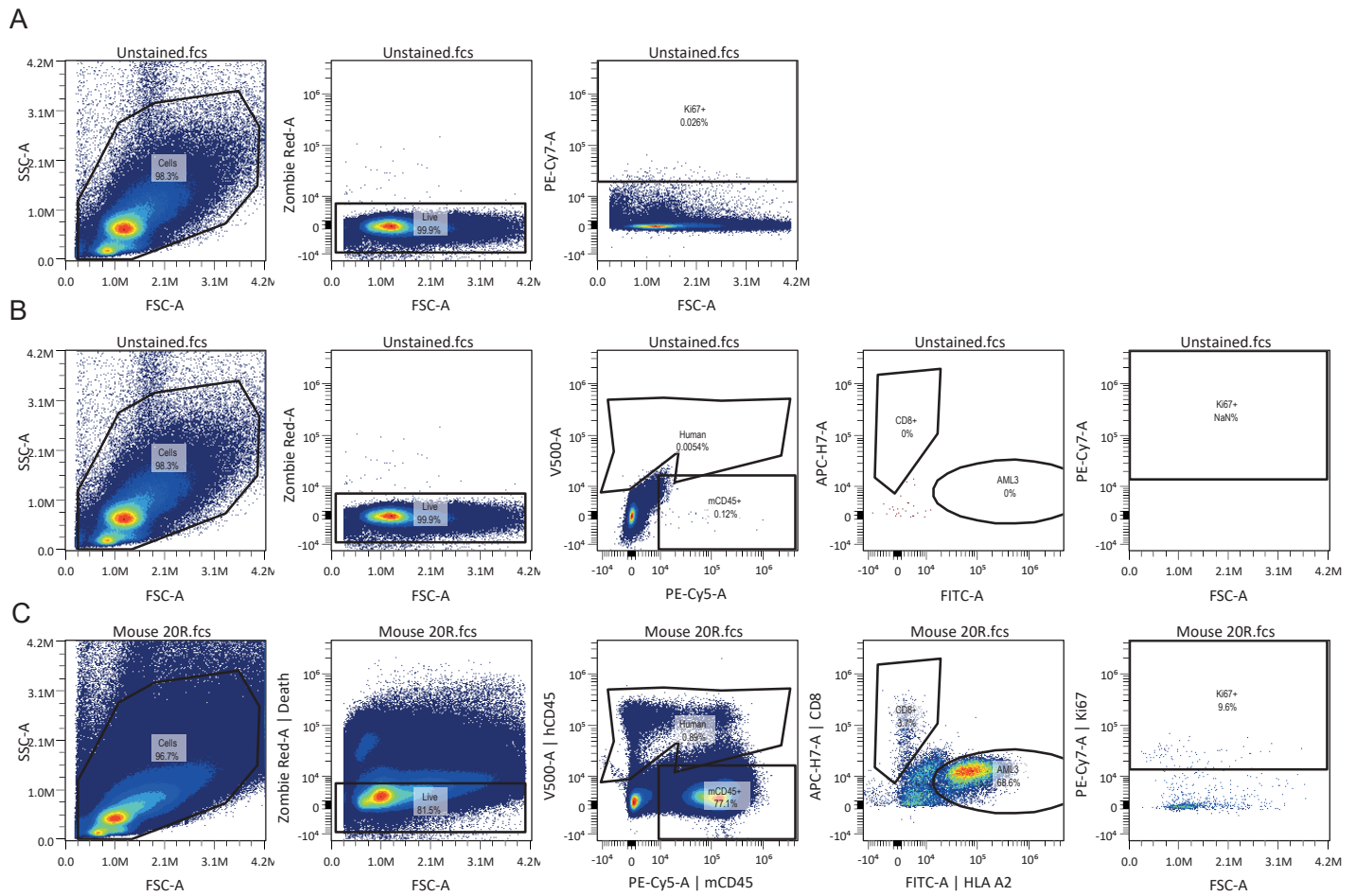


Figure S5

Supplementary Figure 5 Gating strategy for data presented in Figure 4 D and E. **A** Control unstained sample from bone marrow harvested on Day 7 was used to set the gating. ZombieRed staining was used to gate live cells. Human cells were separated via differential mouse versus human CD45 staining. Human cells were gated and CD8⁺ cells were separated from OCI-AML3 cells via HLA-A2/HLA-ABC versus CD8⁺. One representative gating was shown for a mouse stained with indicated markers. **B** Similar to **(A)** gating for day 9 was performed. Extra row (middle) indicates an example for loss of live cells occurring in all the CMV-TCR samples and therefor were excluded from analysis. Samples were measured with Cytex Aurora spectral flow cytometer 3L (Cytekbio) and analyzed with OMIQ.ai (Dotmatics).



Supplementary Figure 6 Gating strategy for data presented in Figure 5 and 6. **A** Unstained sample was used to set the boundaries for the marker stainings. Example shown for Ki67 staining. **B** Control unstained sample was used to set the gating. ZombieRed staining was used to gate live cells. Human cells were separated via differential mouse versus human CD45 staining. Human cells were gated and CD8+ cells were separated from OCI-AML3 cells via HLA-A2/HLA-ABC versus CD8+. **C** Example sample indicating gating on stained sample. ZombieRed staining was used to gate live cells. Human cells were separated via differential mouse versus human CD45 staining. Human cells were gated and CD8+ cells were separated from OCI-AML3 cells via HLA-A2/HLA-ABC versus CD8+. For selected markers, mean fluor intensity (MFI) and percentage positive cells were analysed for CD8+ population and HLA-A2 or HLA-ABC populations. Samples were measured with Cytex Aurora spectral flow cytometer 3L (Cytexbio) and analyzed with OMIQ.ai (Dotmatics).